THE FLOW OVER A BODY IN A CHOKED WIND TUNNEL

AND IN A SONIC FREE-JET

Thesis by

Bernard W. Marschner

In Partial Fulfillment of the Requirements

For the Degree of

Doctor of Philosophy

California Institute of Technology

Pasadena, California

1954

ACKNOWLEDGMENTS

ABSTRACT

The pressure distribution over a double wedge airfoil under free flight conditions with Mach number one is compared with the pressure distribution over the same airfoil in a choked closed wind tunnel and in a sonic free-jet.

The computation is carried out as a development with respect to a parameter which indicates the deviation from free flight conditions with Mach number one. The results are of interest for the question of wind tunnel wall influences. It is found that the deviations of the pressure distribution for a sonic free-jet from the distribution in an infinite air flow are somewhat larger than the deviations in a closed wind tunnel under choked flow conditions. For a specific example of a wedge of a length of 13% of the tunnel height and a thickness ratio of 10%, the deviation of the pressure distribution does not go much beyond the usual experimental scatter.

The results are quite encouraging for the application of closed throat wind tunnels in transonic testing although the axial symmetric case may not show entirely the same desirable behavior.

TABLE OF CONTENTS

I. INTRODUCTION

Generally the test results obtained in a solid wall wind tunnel under conditions at and close to choking are considered somewhat unreliable. It is believed that data obtained for the flow over a body would be greatly distorted once the local supersonic region on the body grows to the extent that it approaches the wind tunnel walls. In a recent theoretical investigation (Ref. 1) it was shown that a flow under choking conditions will have in the vicinity of the model a close resemblance to a flow with a free stream Mach number one, if the ratio between tunnel width and model height is sufficiently large. The important question to be examined is the order of magnitude of the flow deviation. If for a physically reasonable ratio of wind tunnel to model size this deviation is within limits which are acceptable from a technical point of view, then it would be possible to utilize present closed test sections in an extended Mach number range. For this reason the present paper determines numerical data for the specific example of a double wedge airfoil in a choked closed wind tunnel and also in a sonic free-jet of finite width. Of specific interest is a comparison of the pressure distributions obtained under these conditions and those in a free stream of Mach number one. This latter case is available in Ref. 2.

II. FORMULATION OF THE BOUNDARY VALUE PROBLEM

Figure 1 shows a double wedge airfoil in a closed wall wind tunnel under choking conditions. The sonic line CO extends with a downstream slope from the model to the wall. The flow upstream of the model is independent from the downstream portion. As the structure of this flow field has been described previously (Ref. 2), it is mentioned only that from the shoulder of the wedge a fan of rarefaction waves will extend out into the flow. Some of these Mach waves will end at the sonic line while those further downstream end at the wind tunnel wall. The Mach wave DO which reaches the sonic line last, i.e., the Mach wave whose point of intersection with the sonic line lies at the wall, will be referred to as the limiting characteristic; it limits that part of the supersonic region which influences the subsonic region.

The representation of this flow pattern in the hodograph plane is shown in Fig. 2. Corresponding points in the physical plane (Fig. 1) and in the hodograph plane (Fig. 2) have the same notations. The zero streamline starts at infinity with the choking Mach number and goes to the stagnation point at the nose of the wedge, then it follows the side of the wedge to the shoulder. At the shoulder it undergoes a Prandtl-Meyer expansion, the line CD is referred to as the shoulder characteristic. The wall streamline starts with the choking Mach number and increases to the sonic speed; as its slope is zero, it maps along the u- axis in the hodograph plane.

The question whether this is the only possible formulation of the boundary value problem in the hodograph plane is very difficult to answer.

One may consider the above formulation as tentative, then the results of the computations will demonstrate whether one obtains a physically plausible flow pattern. A strong support of the present formulation is the fact that it can be obtained from the formulation of the flow with Mach number one which is known to give a result of physical significance, by a continuous deformation of the boundaries.

The wedge in a sonic free-jet is shown in Fig. 3. In this case all streamlines begin with the sonic velocity. At the boundary streamline sonic speed prevails throughout the flow field and the zero streamline goes to the stagnation point on the nose of the wedge and then follows the side of the wedge. The concept of limiting characteristic and shoulder characteristic also applies in this case and the corresponding hodograph representation of this flow in Fig. 4 is easily understood.

As usual the hodograph equation will be reduced by the transonic approximation to the so-called Tricomi equation. The above boundary value problems are of the type investigated by Tricomi (Ref. 3). An attempt to use Tricomi's procedure in construction of the solution led to very cumbersome computations. For the solutions to be presented the following point of view is of importance. In the case to be calculated the models will be small in comparison to the height of the wind tunnel hence the choking Mach number will be close to one. Therefore the attempt to develop the flow field with respect to the deviation of the choking Mach number from one appears promising. For this purpose an approach particularly well suited has been given in Ref. 1. The details will be presented after the necessary system of particular solutions have been introduced.

III. BASIC EQUATIONS

The equations that are used in the subsequent analysis are introduced in the following. The notations utilized are:

Φ velocity potential

ψ stream function

φ potential transformed by Legendre's transformation

a speed of sound

p pressure

$\overline{\rho}$ density

ρ^* density at the sonic speed

x, y cartesian coordinates in the physical plane

w^* the sonic velocity

w absolute value of velocity vector

θ inclination of velocity vector with x axis

u, v velocity components in x and y direction

γ ratio of specific heats (1.4)

In the actual computations only the density at the sonic speed will occur. It can be placed equal to one without loss of generality.

The differential equation for the potential in two-dimensional isentropic compressible flow is given by:

$$\left(1 - \frac{u^2}{a^2}\right) \Phi_{xx} - \frac{2uv}{a^2} \Phi_{xy} + \left(1 - \frac{v^2}{a^2}\right) \Phi_{yy} = 0 \tag{3.1}$$

Applying the Legendre transformation and utilizing polar coordinates we obtain the form:

$$\varphi_{ww} + \frac{1}{w^2}\left(1 + \frac{w^2}{a^2}\right) \varphi_{w\theta} + \frac{1}{w^2}\left(1 - \frac{w^2}{a^2}\right) \varphi_{\theta\theta} = 0 \tag{3.2}$$

A new variable is introduced by the equation

$$w = w^* \left[1 + (\gamma - 1)^{-\frac{1}{3}} \eta \right] \tag{3.3}$$

The line $\eta = 0$ coincides with the sonic line. With certain simplifications known from the derivation of the transonic similarity law the following equation is obtained

$$\varphi_{\eta\eta} - \eta \varphi_{\theta\theta} = 0 \tag{3.4}$$

In a similar fashion the equation for the stream function is obtained.

$$\psi_{\eta\eta} - \eta \, \psi_{\theta\theta} = 0 \tag{3.5}$$

Between the stream function and the transformed potential there exist the relations Ref. 6.

$$\psi_w = \bar{\rho} \left[\varphi_{w\theta} - \frac{\varphi_\theta}{w} \right] \tag{3.6}$$

$$\psi_\theta = \bar{\rho} \left[w \, \varphi_w + \varphi_{\theta\theta} \right] \tag{3.7}$$

In the present approximation these equations reduce to

$$\psi = \rho^* \, \varphi_\theta \tag{3.8a}$$

and with ρ^* equal to one

$$\psi = \varphi_\theta \tag{3.8b}$$

The coordinates in the physical plane are found to be:

$$x = \frac{1}{w^*} \left[\varphi_w \cos\theta - \varphi_\theta \frac{\sin\theta}{w} \right] \tag{3.9}$$

$$y = \frac{1}{w^*}\left[\varphi_w \sin\theta + \varphi_\theta \frac{\cos\theta}{w} \right]$$

$$\text{(3.10)}$$

Within the present approximation

$$\chi = \frac{(\gamma+1)^{-\frac{1}{3}}}{w^*} \varphi_\eta$$

$$\text{(3.11)}$$

$$y = \frac{1}{w^*} \varphi_\theta$$

$$\text{(3.12)}$$

Equations (3.4) and (3.5) are of the form discussed by Tricomi (Ref. 3).

The map of the wedge in a solid wall tunnel in the transformed hodograph (η, θ) plane is presented in Fig. 5 and of the sonic free-jet case in Fig. 6. The notation of corresponding points is the same as in Figs. 1, 2, 3, and 4.

IV. SYSTEMS OF PARTICULAR SOLUTIONS

Two systems of particular solutions of Eq. (3.5) are of importance in this analysis.

The first system is obtained by a product hypothesis of Eq. (3.5).

$$\psi = g(\eta, m) \sin \frac{m \pi \theta}{\theta_0} \tag{4.1}$$

from which the following equation for $g(\eta, m)$ is obtained.

$$\frac{d^2 g(\eta, m)}{d \eta^2} + \left(\frac{m \pi}{\theta_0}\right)^2 \eta \, g(\eta, m) = 0 \tag{4.2}$$

The functions $g(\eta, m)$ can be expressed in terms of Bessel functions.

$$g(\eta, m) = \sqrt{\frac{|\eta|}{\left(\frac{3}{2}\theta_0\right)^{\frac{2}{3}}}} \; Z_{\frac{1}{3}} \left\{ m \pi \left[\frac{\eta}{\left(\frac{3}{2}\theta_0\right)^{\frac{2}{3}}} \right]^{\frac{3}{2}} \right\} \tag{4.3}$$

where $Z_{\frac{1}{3}}$ indicates any linear combination of Bessel functions of the order 1/3.

For future applications that combination of Bessel functions will be used which tends to zero as η tends to $-\infty$. Then

$$g(\eta, m) = e^{\frac{2 i \pi}{3}} \sqrt{\frac{|\eta|}{\left(\frac{3}{2}\theta_0\right)^{\frac{2}{3}}}} \; H_{\frac{1}{3}}^{(1)} \left\{ m \pi i \left[\frac{|\eta|}{\left(\frac{3}{2}\theta_0\right)^{\frac{2}{3}}} \right]^{\frac{3}{2}} \right\}, \quad \eta < 0 \tag{4.4}$$

where $H_{\frac{1}{3}}^{(1)}$ is a Hankel function of the first kind of order 1/3. The representation in the supersonic region is then

$$g(\eta, m) = \frac{2}{3} \sqrt{\frac{\eta}{\left(\frac{3}{2}\theta_0\right)^{\frac{2}{3}}}} \left[J_{\frac{1}{3}} \left\{ m \pi \left[\frac{\eta}{\left(\frac{3}{2}\theta_0\right)^{\frac{2}{3}}} \right]^{\frac{3}{2}} \right\} + J_{-\frac{1}{3}} \left\{ m \pi \left[\frac{\eta}{\left(\frac{3}{2}\theta_0\right)^{\frac{2}{3}}} \right]^{\frac{3}{2}} \right\} \right], \quad \eta > 0 \tag{4.5}$$

where $J_{\pm\frac{1}{3}}$ are Bessel functions of order 1/3. We note for future use:

$$\frac{dg(\eta,m)}{d\eta} = \frac{3}{2}\frac{m\pi}{(\frac{3}{2}\theta_{o})^{\frac{2}{3}}}\ i^{\frac{5}{3}}\ H_{\frac{2}{3}}^{(1)}\left\{m\pi i\left[\frac{|\eta|}{(\frac{3}{2}\theta_{o})^{\frac{2}{3}}}\right]^{\frac{3}{2}}\right\}\qquad \eta < 0 \qquad\qquad (4.6)$$

where $H_{\frac{2}{3}}^{(1)}$ is a Hankel function of the first kind of order 2/3.

To derive the other system of particular solutions it is convenient to introduce a new set of independent variables.

$$\xi = \eta \Big/ \left(\tfrac{3}{2}\,\theta\right)^{\frac{2}{3}} \qquad\qquad (4.7)$$

and

$$\rho = -\eta^{3} + \left(\tfrac{3}{2}\,\theta\right)^{2} \qquad\qquad (4.8)$$

A plot of lines of constant ξ and ρ in the η, θ plane is shown in Fig. 7. Transforming to ξ, ρ coordinate system the equation for the stream function becomes:

$$\frac{(1-\xi^{3})^{2}}{\xi}\psi_{\xi\xi} - \frac{5}{2}\xi(1-\xi^{3})\psi_{\xi} + \frac{1}{16}\psi = 9\rho^{2}\psi_{\rho\rho} + \frac{21}{2}\psi_{\rho} + \frac{1}{16}\psi \qquad (4.9)$$

By the product hypothesis:

$$\psi = g(\rho)\,G(\xi) \qquad\qquad (4.10)$$

the following two differential equations are obtained:

$$9\rho^{2}\frac{d^{2}g(\rho)}{d\rho^{2}} + \frac{21}{2}\rho\frac{dg(\rho)}{d\rho} + \left(-\lambda + \frac{1}{16}\right)g(\rho) = 0 \qquad (4.11)$$

and

$$\frac{(1-\xi^{3})^{2}}{\xi}\frac{d^{2}G}{d\xi^{2}} - \frac{5}{2}\xi(1-\xi^{3})\frac{dG}{d\xi} + \left(-\lambda + \frac{1}{16}\right)G = 0 \qquad (4.12)$$

λ is a constant which is introduced by the separation of variables. The solution to the first equation is

$$g(\rho) = \rho^{-\frac{1}{12} \pm \frac{1}{3}\sqrt{\lambda}} \qquad\qquad (4.13)$$

The self adjoint form of Eq. (4.12) is

$$\frac{d\left\{(1-\xi^3)^{\frac{5}{6}}\frac{dG}{d\xi}\right\}}{d\xi} + \frac{(-\lambda + \frac{1}{16})}{(1-\xi^3)^{\frac{7}{6}}}\, G = 0 \tag{4.14}$$

The differential equation, Eq. (4.12), is closely connected to a hypergeometric differential equation as discussed in Appendix Ia.

For a given value of λ there exist two linearly independent solutions $G(\xi)$. One can choose them such that the arising functions ψ are symmetric or antisymmetric with respect to the line $\xi = -\infty$. Accordingly the functions $G(\xi)$ may be differentiated by a superscript (s) or (a) respectively. As the functions $G^{(a)}$ and $G^{(s)}$ depend upon ξ and also upon λ they will be written as $G^{(a)}(\xi,\lambda)$ and $G^{(s)}(\xi,\lambda)$.

Formulae for the functions $G^{(a)}(\xi,\lambda)$ and $G^{(s)}(\xi,\lambda)$ are presented in Appendix Ia. The functions $G(\xi,\lambda)$ are tabulated for special values of λ in Ref. 4. A different notation is used in the tables of Ref. 4 and is listed for information:

Harvard Tables (Ref. 4)	Present Paper
x	ξ
y	$G(\xi,\lambda)$
y'	$dG/d\xi$
w	$(-\xi)^{-\frac{3}{2}}$

The function y for K = 0, 2, 4, 6, ... in Ref. 4 are in our notation to $G^{(s)}(\xi,\lambda)$ with $\lambda = \left(\frac{3}{4} + 3h\right)^2$ for h = 0, 1, 2, ... Likewise the functions y for K = 1, 3, 5, ... are $G^{(a)}(\xi,\lambda)$ with $\lambda = \left(\frac{9}{4} + 3h\right)^2$ for h = 0, 1, 2, ...

V. SELECTION OF THE PARAMETERS m AND λ

Both m and λ in Eqs. (4.1) and (4.12) were introduced in a
general manner and may assume any value. For the present paper only
special values of these parameters are required.

For the particular solution Eq. (4.1) and condition $\psi = 0$ will
be imposed along the lines $\theta = 0$ and $\theta = \theta_o$. It is seen directly
from Eq. (4.1) that m will then be an integral number.

In the application of the other particular solution Eq. (4.10)
several families will be utilized. The boundary condition common to
both families will be $\psi = 0$ along the line $\xi = -\infty$. The line
$\xi = -\infty$ corresponds to $\theta = 0$. The other prescription will be $\psi = 0$
along a line $\xi = C_2$ where C_2 is a constant whose choice will be settled
later. With this prescription of boundary conditions on ψ Eq. (4.12)
has the familiar form of an eigen value problem. The only deviation
from the classical type of eigen value problem is that the coefficient
of $G(\xi,\lambda)$ in Eq. (4.14) changes sign as ξ passes through zero. As
stated in Ref. 1 the eigen functions $G(\xi,\lambda)$ have the following properties:

a. The eigen functions are orthogonal

b. The eigen values are positive or negative real numbers

c. The system of eigen functions is complete

The eigen values will be arranged according to the magnitude and are
denoted by: $\lambda_{-h}, \cdots \lambda_{-2}, \lambda_{-1}, \lambda_1, \lambda_2, \cdots \lambda_h$
where the negative and positive subscripts refer to negative and positive
eigen values respectively. The eigen functions belonging to these eigen
values are introduced:

$$G(\xi,\lambda_{-h}) \cdots G(\xi,\lambda_{-1}), \quad G(\xi,\lambda_1), \cdots G(\xi,\lambda_h)$$

The relations of orthoganality are derived in the standard manner and are:

$$\int_{C_1}^{C_2} \frac{\xi}{(1-\xi^3)^{\frac{7}{6}}} G(\xi, \lambda_h) G(\xi, \lambda_k) d\xi = 0 \qquad \text{for} \quad h \neq k \qquad (5.1)$$

$$\int_{C_1}^{C_2} (1-\xi^3)^{\frac{5}{6}} \frac{dG(\xi, \lambda_h)}{d\xi} \frac{dG(\xi, \lambda_k)}{d\xi} d\xi = 0 \qquad \text{for} \quad h \neq k \qquad (5.2)$$

Utilizing the indicated ordering of the eigen values the following notation for the particular solutions of Eq. (4.10) are introduced:

$$\psi_{I_h} = G\left\{\xi, \lambda_h\right\} \rho^{-\frac{1}{12} + \frac{1}{3}\sqrt{\lambda_h}} \qquad (5.3a)$$

$$\psi_{II_h} = G\left\{\xi, \lambda_h\right\} \rho^{-\frac{1}{12} - \frac{1}{3}\sqrt{\lambda_h}} \qquad (5.3b)$$

$$\psi_{III_h} = G\left\{\xi, \lambda_{-h}\right\} \rho^{-\frac{1}{12}} \cos\left\{\frac{\nu_h}{3} \log \frac{\rho}{\rho_0}\right\} \qquad (5.3c)$$

$$\psi_{IV_h} = G\left\{\xi, \lambda_{-h}\right\} \rho^{-\frac{1}{12}} \sin\left\{\frac{\nu_h}{3} \log \frac{\rho}{\rho_0}\right\} \qquad (5.3d)$$

where $\nu_h = \sqrt{-\lambda_h}$ and ρ_0 is an arbitrary constant. The functions $G(\xi, \lambda_h)$ are represented in terms of hypergeometric functions and can be found in Appendix Ia.

The first family of the particular solutions of the form Eq. (4.10) is obtained by choosing $C_2 = 0$ which is the prescription of $\psi = 0$ along the sonic line. This prescription on the sonic line is used in Tricomi's memoir (Ref. 3). From the formulas for $G\left\{\xi, \lambda_h\right\}$ in Ref. 1, the eigen values are determined to be:

‌

$$\lambda_h = \left\{ \frac{11}{4} + 3h \right\}^2$$

(5.4)

The second family of particular solution of Eq. (4.12) arises if one tries to represent certain solutions of the Tricomi equation, Eq. (3.5), in a region OB'CD in Fig. 8. This region is bounded by $\xi = -\infty$, $\rho = \rho_c$ the characteristic CD, and the characteristic OD. Along the lower limit of $\xi = -\infty$ the boundary condition $\psi = 0$ is prescribed. If the characteristic CD is considered a boundary then the upper limit of ξ is a function of ρ . This situation can be remedied by including consideration of the area bounded by the characteristic CD, the characteristic DG, and the line $\rho = \rho_c$, CF ; the shaded area indicated in Fig. 8. Since the boundary condition $\psi = 0$ is prescribed along the characteristic CD the differential equation will be satisfied everywhere in the region GDOB'CF when $\psi = 0$ is prescribed in the region GDCF. Draw a line $\xi = C_2$ in Fig. 8, i.e., OD'D" and the line $\rho = \rho_o$ through point A. Then in the region AB'CFD"D'E of Fig. 8 the upper limit of ξ is $\xi = C_2$. The boundary condition $\psi = 0$ along $\xi = C_2$ is imposed establishing an eigen value problem and a system of eigen functions which depend on the choice of C_2 can be obtained. The choice of C_2 was arbitrary and the values of ρ_o become smaller when C_2 approaches one. Thus in order to represent a solution with the boundary value of $\psi = 0$ along OBBCD the system of particular solutions obtained by prescribing $\psi = 0$ along $\xi = C_2$ and letting C_2 tend to one can be used. Some aspects of this limiting process will be discussed in the next section. The positive eigen values obtained by the use of this limiting process and the formulae for $G(\xi, \lambda_h)$ in Ref. 1 are:

$$\lambda_h = \left(\frac{9}{4} + 3h\right)^2 \qquad h = 0, 1, 2, \cdots \qquad (5.5)$$

The negative eigen values form a continuous spectrum, but are without importance in the present application.

For the specific eigen values given in Eq. (5.5) the following notation is introduced for the particular solutions given in Eq. (5.3):

$$\Psi_{I_h} = \psi_{I_h} \qquad (5.6a)$$

$$\Psi_{II_h} = \psi_{II_h} \qquad (5.6b)$$

$$\Psi_{III_h} = \psi_{III_h} \qquad (5.6c)$$

$$\Psi_{IV_h} = \psi_{IV_h} \qquad (5.6d)$$

for

$$\lambda_h = \left(\frac{9}{4} + 3h\right)^2$$

VI. THE LIMITING PROCESS THAT c_2 TENDS TO ONE

By means of the detailed formulae for the eigen functions $G(\xi,\lambda)$ given in Appendix Ia and in Ref. 1, it is possible to determine the eigen values λ under the conditions that C_2 is close to one and then carry out the limiting process that C_2 tends to one. Details of this limiting process are shown in Ref. 1 where it is found that as C_2 tends to one the positive eigen values tend to discrete numbers while the negative eigen values will occur at smaller and smaller intervals. In the limit as C_2 tends to one the spectrum of the negative eigen values is continuous. The process as C_2 tends to one is similar to that of a Fourier series for which the upper limit of the interval tends to infinity and a Fourier integral arises. One might be tempted to replace the condition that $G(\xi,\lambda)=0$ at $\xi = C_2$ as C_2 tends to one by the requirement that $G(\xi,\lambda)=0$ for C_2 equaling one. Such a formulation would contradict the requirement of Tricomi's investigation of the boundary value problem (Ref. 3). In some cases, the boundary in the vicinity of the origin coincides with the line $C_2 = 1$ and no boundary conditions are prescribed along this line. The idea of the limiting process will be retained in the determination of the eigen values and hence in the definition of the eigen functions. It would be very desirable from a mathematical point of view if the system of particular solutions and their properties could be derived by considerations that avoid this limiting process in the formulation of the eigen value problem, and if a formula equivalent to Fourier's integral formula could be derived directly. To the author's knowledge such an approach has not yet been carried out.

VII. THE ROLE OF THE SOLUTIONS $\psi_{\mathbb{I}_h}$
IN THE PRESENT BOUNDARY VALUE PROBLEM

Both the flow in the closed wind tunnel and in the sonic free-jet can be treated to a large extent in the same manner. Consider the line $\rho = \rho_o$ through the point A in Fig. 5 and the point E in Fig. 6, this line divides the domain into two regions, the inner region $(\rho < \rho_o)$ and the outer region $(\rho > \rho_o)$.

Introduce a system of functions $\overline{\psi}_h$ which consist of a singular portion given by one of the functions $\psi_{\mathbb{I}_h}$ and another portion $\widetilde{\psi}_h$ which is regular in the sense required in Tricomi's uniqueness and existence proof (Ref. 4).

$$\overline{\psi}_h = \psi_{\mathbb{I}_h} + \widetilde{\psi}_h \qquad (7.1)$$

The functions $\overline{\psi}_h$ are required to fulfill the boundary condition $\psi = 0$ along the surface of the body ABCD (Fig. 8). Then as shown in Appendix I, any solution which fulfills for $\rho > \rho_o$ the differential equation, Eq. (3.5), and the boundary condition $\psi = 0$ can be represented by a superposition of the function $\overline{\psi}_h$. It is then possible to express the solution in both cases for $\rho > \rho_o$ by a series with undetermined coefficients of the form

$$\psi = \sum_{h=0}^{\infty} C_h \overline{\psi}_h \qquad (7.2)$$

For small values of ρ_o the later terms (h = 1, 2, ...) will appear as a perturbation on the first term (h = 0). In the cases under consideration, the first term will represent the flow with a Mach number one over the given body. The perturbation terms represent the effect of the

change of the boundary conditions at a distance from the body. This change of the boundary conditions consists in the solid wall case as a shift of the singularity from the point O where it is located in the free stream case, to the point A in Fig. 5. Along AO the boundary condition ψ = constant will be prescribed. In the case of the sonic free-jet, the location of the singularity remains unchanged, but the condition ψ = constant is imposed along OE in Fig. 6.

The present procedure is still unsatisfactory since by a superposition of the perturbation terms (i.e., by $\overline{\psi}_h$; $h = 1, 2, \cdots$) the length of the sides of the wedge will in general be changed. To be more specific, if one superimposes in the hodograph plane certain expressions ψ on each other then in the physical plane the coordinates of the points which would be found for the particular solutions ψ are additive. The particular solutions $\overline{\psi}_h$ will be constructed so that the nose of the wedge lies at the origin of the x.y system in the physical plane. For the shoulder of the wedge the expressions $\overline{\psi}_h$ will in general give a value of x different from zero. Now form a linear combination of the $\overline{\psi}_h$ $(h=1,2 \ldots)$ with the $\overline{\psi}_o$, i.e., with the solution of the basic flow, such that in these combinations the value of x at the shoulder is zero. This is always possible since in the basic flow the length of the wedge side is different from zero. Thus the following combination will be used.

$$\overline{\overline{\psi}}_h = \overline{\psi}_h + b_h \overline{\psi}_o \qquad h = 1, 2, 3, \cdots \qquad (7.3)$$

where b_h is a constant chosen in such a manner that x at the shoulder obtained from the $\overline{\overline{\psi}}_h$ (h = 1, 2, ...) will vanish. Then the most general solution which fulfills all of the conditions at the surface of the body can be written

$$\psi = C_o \, \overline{\psi}_o + \sum_{h=1} C_h \, \overline{\overline{\psi}}_h \qquad (7.4a)$$

or in another form

$$\psi = C_o \left\{ \psi_{II_o} + \overline{\psi}_o \right\} + \sum_{h=1} C_h \left\{ \psi_{II_h} + b_h \psi_{II_o} + \overline{\psi}_h \right\} \qquad (7.4b)$$

The treatment of the inner region $\rho < \rho_o$ depends upon the boundary conditions prescribed. The boundary conditions in this region are non-homogeneous with ψ assuming a constant value in Fig. 5 along AO and in Fig. 6 along EO. The representation of the inner solution will be split into a portion which fulfills the non-homogeneous boundary condition just mentioned and a portion which has $\psi = 0$ along the boundary. Since the lines AO and OE are lines $\xi = $ constant, the non-homogeneous portion will be found from Eq. (4.10) with $\sqrt{\lambda_h} = -\frac{1}{4}$. These particular solutions will be denoted by H(ξ). The details of this non-homogeneous portion are presented in Appendix II. The homogeneous portion is formed by solutions of the form of Eq. (4.10) which fulfill the boundary condition $\psi = 0$ along $\theta = 0$ (i.e., along $\xi = -\infty$) and along OA or OE in Figs. 5 and 6 respectively. (This can be written as $\psi = 0$ along $\xi = C_\lambda$. In the case of the free-jet $C_\lambda = 0$ while in the closed tunnel an application of a limiting process of $C_\lambda \to 1$ must be utilized.) Thus the inner solution can be represented by the non-homogeneous portion and a superposition of the expressions

$$\psi = \sum C_{I_h} \psi_{I_h} + \sum C_{II_h} \psi_{II_h} + \sum C_{IV_h} \psi_{IV_h} \qquad (7.5a)$$

for the closed tunnel. For the closed tunnel obviously the expressions ψ_{II_h} must be excluded from the representation of the inner region for the closed tunnel since they would introduce a singularity at the origin.

Also the expressions ψ_{III_h} and ψ_{IV_h} are singular at the origin. However by the superposition in the limit $c_1 \to 1$ these singularities cancel out. Some more of the details are to be found in Ref. 1.

In the free-jet case the point 0 is singular since ψ jumps at this point. Point 0 in Fig. 6 represents the free-jet at some distance upstream of the model. It can be seen that ψ varies only between the value zero and some finite values at the surface of the free-jet. If any singularity ψ_{II_h} would be included at the point 0, ψ would assume values beyond any limit, therefore the functions ψ_{II_h} can not be admitted and the inner solution will contain ψ_{I_h} only. ψ_{III_h} and ψ_{IV_h} do not exist in this case as the inner region is entirely subsonic.

$$\psi = \sum C_{I_h} \, \psi_{I_h} \tag{7.5b}$$

for the sonic free-jet.

The coefficients C_{I_h} , C_{III_h} , C_{IV_h} and C_h will then be found by matching the inner and outer representations along the line $\rho = \rho_o$.

An essential simplification arises if consideration is limited to cases where ρ_o is very small, i.e., cases where the tunnel height is large relative to the dimensions of the wedge. Then when matching the inner and outer representations along the line $\rho = \rho_o$ the term $\bar{\psi}_{II_h}$ will dominate in the expression for $\bar{\psi}_h$ in Eq. (7.1) near the vicinity of the matching curve $\rho = \rho_o$. Thus in the matching process only the term containing $\bar{\psi}_{II_h}$ need be considered in the representation of the outer solution.

$$\psi = \sum C_{II_h} \, \bar{\psi}_{II_h} \tag{7.6}$$

The program for the computations is:

    a. Determination of the expression $\overline{\overline{\psi}}_h$. To find the lowest order correction for a very wide tunnel only $\overline{\overline{\psi}}_i$ is needed.

    b. Matching of the inner and outer representations.

    c. Determination of the change of the pressure coefficient caused by the perturbation term.

VIII. FULFILLMENT OF THE BOUNDARY CONDITIONS
AT THE CLOSED WIND TUNNEL WALL AND AT THE SURFACE OF THE FREE-JET

A. The sonic Free-Jet Case

In this case the line $\rho = \rho_o$ which in Fig. 6 separates the domain under consideration into the inner region $\rho < \rho_o$ and the outer region $\rho > \rho_o$ passes through point E. As explained in Section VII the outer representation will be given by

$$\psi = \sum_h \beta_h \, \overline{\overline{\psi_h}} \qquad (\, h = 0, 1, 2, \cdots \qquad) \tag{8.1}$$

where β_h are suitable coefficients. In the terms $\overline{\overline{\psi_h}}$ in Eqs. (7.3) and (7.1) the expressions ψ_{II_h} will prevail for small values of ρ_o. Then ψ in the outer region in the vicinity of $\rho = \rho_o$ is represented by

$$\psi = \sum_h \beta_h \, \rho^{-\frac{5}{6}-h} \, G\left\{ \xi, \left(\tfrac{9}{4} + 3h \right)^2 \right\} \qquad (h = 0, 1, 2, \cdots) \tag{8.2}$$

In the following we shall put

$$\beta_h = b_h \, \rho_o^{-\frac{5}{6}+h} \tag{8.3}$$

and thus obtain for the outer representation:

$$\psi = \sum_h b_h \left(\frac{\rho}{\rho_o} \right)^{-\frac{5}{6}-h} G\left\{ \xi, \left(\tfrac{9}{4} + 3h \right)^2 \right\} \qquad (h = 0, 1, 2, \cdots) \tag{8.4}$$

As discussed in Section VII and with the eigen values for the case of $c_2 = 0$ given in Eq. (5.4) and with $C_{I_h} = a_h \, \rho_o^{-\frac{5}{6}-h}$ the inner representation can be written as

$$\psi = H(\xi) + \sum_h a_h \left(\frac{\rho}{\rho_o}\right)^{\frac{5}{6}+h} G\left\{\xi, \left(\frac{11}{4}+3h\right)^2\right\} \quad (h=0,1,2,\cdots) \tag{8.5}$$

Along the curve $\rho = \rho_o$ the ψ and ψ_ρ are matched for the two representations Eq. (8.4) and Eq. (8.5). For the details of the matching process the reader is referred to Appendix II. The results for the first two coefficients of the outer region for sonic free-jet case are

$$b_o = .395 \tag{8.6a}$$

$$b_1 = - .290 \tag{8.6b}$$

As this paper is concerned only with the details of the flow near the surface of the body and also for cases of small ρ_o these are the only coefficients that will be required.

B. The Closed Wind Tunnel Case

In this case the line $\rho = \rho_o$ passes through the point A of Fig. 5 and the outer representation is the same as in the free-jet case as given in Eq. (8.4) (naturally with different values of b_h).

And as discussed in Section VII the inner representation is given by:

$$\psi = H(\xi) + \sum_h C_{I_h} \psi_{I_h} + \sum_h C_{III_h} \psi_{III_h} + \sum_h C_{IV_h} \psi_{IV_h} \tag{8.7a}$$

or

$$\psi = H(\xi) + \sum_h a_h \left(\frac{\rho}{\rho_o}\right)^{\frac{2}{3}+h} G\left\{\xi, \left(\frac{9}{4}+3h\right)^2\right\}$$
$$+ \sum_h C_h \left(\frac{\rho}{\rho_o}\right)^{-\frac{1}{12}} \cos\left\{\frac{\nu h}{3}\log\frac{\rho}{\rho_o}\right\} G(\xi,\lambda) + \sum_h d_h \left(\frac{\rho}{\rho_o}\right)^{-\frac{1}{12}} \sin\left\{\frac{\nu h}{3}\log\frac{\rho}{\rho_o}\right\} G(\xi,\lambda) \tag{8.7b}$$

Again, as in the sonic free-jet case, the inner and outer representation and their normal derivative are matched along the line $f = f_o$. From the Appendix II one obtains for the closed tunnel case

$$b_o = .586 \tag{8.8a}$$

$$b_1 = .611 \tag{8.8b}$$

IX. DETERMINATION OF THE PARTICULAR SOLUTION $\overline{\psi}_I$

A detailed description of this part of the computation is presented in Appendix III. In this section only the main features will be presented so that the results can be discussed and the figures interpreted.

First the function, $\overline{\psi}_{I_i}$, must be determined. This function is the solution of the Tricomi equation which fulfills the boundary condition $\psi = 0$ along the boundary OABCD of Fig. 8 and furthermore has a singularity at the origin given by

$$\psi = \rho^{-\frac{4}{6}} \; G\left\{ \xi, \; \left(\frac{q}{4} + 3\right)^2\right\} \tag{9.1}$$

An expression which has the proper singularity at the origin and fulfills the boundary conditions $\psi = 0$ along $\theta = 0$ and $\theta = \theta_o$ is obtained by an image system of singularities given by Eq. (9.1) spaced along the θ axis at intervals of $2\theta_o$. This part of the solution is denoted by $\overline{\psi}_I^{(\omega)}$.

This system $\overline{\psi}_I^{(\omega)}$ does not satisfy the conditions along the shoulder characteristic CD. The value of the stream function induced by $\psi_I^{(\omega)}$ along the shoulder characteristic is presented in Fig. 10. To fulfill the condition along CD a system of Chapligin solutions Eq. (4.1) is introduced. Coefficients of the Chapligin solutions are chosen to cancel the values of stream function induced by the image system along the shoulder characteristic. How close this superimposed system of Chapligin solutions satisfies this condition is indicated by the circled points on Fig. 10.

By this process the desired solution $\overline{\psi}_{I_i}$ is determined. Next the quantities which are of importance for the pressure distribution over

the wedge will be determined. A preliminary step is the calculation of the values of $\overline{\psi_i}$ induced along the limiting characteristic OD in Fig. 8 which are presented in Fig. 11.

For the evaluation of the change of the pressure distribution the x coordinate along the side of the wedge has been calculated. The x coordinate could be obtained by an integration of ψ_θ and ψ_h in the hodograph plane. The way chosen in these computations was to determine first the expression for the transformed potential which belongs to the expressions $\overline{\psi_i}$. The transformed potential and the stream function are connected by Eq. (3.8a) and the x coordinate may be obtained from Eq. (3.11). In obtaining φ for the calculations Eq. (3.8b) is used which has ρ^* set equal to one.

The notation $\overline{\varphi_i}$ will be used for the expression which corresponds to $\overline{\psi_i}$ and correspondingly other notation will be carried over between the transformed potential and the stream function. Fig. 12 shows $\overline{\varphi_{i\eta}}$ along the subsonic part of the wedge and Fig. 17 for the supersonic portion as a function of $\eta / \left(\frac{3}{2} \theta_o \right)^{\frac{2}{3}}$.

As mentioned previously one must superimpose on these expressions such a portion of the basic flow that the location of the shoulder of the wedge does not change. The values of $\overline{\varphi_{o\eta}}$ for the basic flow are presented in Fig. 18 for the subsonic and the supersonic region.

The superimposed $\overline{\overline{\varphi_{i\eta}}}$ determined from the combination of the additional $\overline{\varphi_{i\eta}}$ and the basic $\overline{\varphi_{o\eta}}$ is presented in Fig. 12 and Fig. 17 for the subsonic and supersonic portions of the wedge respectively.

With these calculations completed, all of the necessary computations are completed and we may proceed to evaluate the changes to the pressure distribution for the two cases under consideration.

X. THE CHANGE OF THE PRESSURE DISTRIBUTION

In the previous considerations the singularities at the point 0 in Fig. 8 were determined to be $\Psi_{\mathbb{I}_0}$ for the basic stream function and $\Psi_{\mathbb{I}_0}$ for the superimposed stream function. For a given body in either the sonic free-jet or the closed wind tunnel case a linear combination of these two solutions will arise, it may be given by

$$\psi = \beta_o \, \overline{\psi}_o + \beta_1 \, \overline{\overline{\psi}}_1 \tag{10.1}$$

The quantities β_o and β_1 will be determined in the next section and are connected to b_o and b_1 as given in Eq. (8.3). For the present analysis consider that β_o and β_1 are known and determine the change of η due to the superimposed stream function $\overline{\overline{\psi}}_1$ at a given point x on the surface of the wedge. The x coordinate of the body is given by

$$\chi = \beta_o \, \overline{\varphi}_{o_\eta} + \beta_1 \, \overline{\overline{\varphi}}_{1_\eta} \tag{10.2}$$

where the quantities $\overline{\varphi}_{o_\eta}$ and $\overline{\overline{\varphi}}_{1_\eta}$ are shown in Figs. 12, 13, 17, and 18. In the basic flow:

$$\chi = \beta_o \, \overline{\varphi}_{o_\eta}(\eta, \theta) \tag{10.3}$$

In the flow given by Eq. (10.1) the value of η at the point x on the wedge will be changed by an amount $\triangle \eta$ then:

$$\chi = \beta_o \, \overline{\varphi}_{o_\eta}(\eta + \triangle \eta, \theta) + \beta_1 \, \overline{\overline{\varphi}}_{1_\eta}(\eta + \triangle \eta, \theta) \tag{10.4a}$$

Assuming that $\triangle \eta$ is small, the x coordinate on the wedge for the changed flow will be given by:

$$\chi = \beta_o \left[\overline{\varphi}_{o_\eta}(\eta, \theta_o) + \triangle \eta \, \overline{\varphi}_{o_{\eta\eta}}(\eta, \theta_o) \right] + \beta_1 \, \overline{\overline{\varphi}}_{1_\eta}(\eta, \theta_o) \tag{10.4b}$$

hence combining the last two equations

$$\Delta \eta = - \frac{\beta_1}{\beta_0} \frac{\overline{\overline{\varphi}}_{1\eta}}{\overline{\varphi}_{0\eta\eta}}$$

(10.5a)

The values of $\overline{\varphi}_{0\eta\eta}$ have been calculated and are presented in Fig. 18 and Fig. 19, and the values of $\overline{\overline{\varphi}}_{1\eta}$ are presented in Fig. 12 and Fig. 17. In the expressions for $\overline{\varphi}_{0\eta\eta}$ and $\overline{\overline{\varphi}}_{1\eta}$ certain powers of θ_0 occur and are indicated in the figures.

Since $\overline{\overline{\varphi}}_{1\eta}$ and $\overline{\varphi}_{0\eta\eta}$ are given as functions of η in the basic flow along the side of the wedge, the last equation gives $\Delta\eta$ as a function of the value of η in the basic flow. We are interested in the dependence of $\Delta\eta$ upon the x coordinate. Such a representation can be obtained easily since the dependence of η in the basic flow upon x/L is given. Therefore $\Delta\eta$ may be written in the form

$$\Delta \eta = - \frac{\beta_1}{\beta_0} \left(\frac{3}{2} \theta_0 \right)^{-\frac{4}{3}} F\left(\frac{x}{L} \right)$$

(10.5b)

The auxiliary function F(x/L) has been plotted in Fig. 20 and Fig. 21. The x coordinate of the wedge $\beta_0 \overline{\varphi}_{0\eta}$ has been made dimensionless with the overall length of the wedge L. For future use it is noted that the overall length of the wedge L is given by

$$L = 2.47 \, \beta_0 \left(\frac{3}{2} \theta_0 \right)^{-\frac{4}{3}} \frac{(\gamma+1)^{\frac{1}{3}}}{w^*}$$

(10.6)

XI. INFLUENCE OF THE TUNNEL WALL
ON THE PRESSURE DISTRIBUTION OVER THE BODY

The boundary condition of $\psi = 1$ imposed along OE and OA in Fig. 5 and Fig. 6 specifies that the half height of the closed wind tunnel or sonic free-jet is $\frac{1}{w^*}$. From Eq. (10.3) we find for general tunnel height H, remembering that ρ^* was assumed to be one.

$$\beta_0 = b_0 \, \rho_0^{\frac{5}{6}} \, \frac{H}{2} \, w^* \tag{11.1}$$

$$\beta_1 = b_1 \, \rho_0^{-\frac{4}{6}} \, \frac{H}{2} \, w^* \tag{11.2}$$

and from Eq. (10.6)

$$\beta_0 = \frac{w^* \, L \, (\gamma+1)^{-\frac{1}{3}}}{2.47 \left(\frac{3}{2} \theta_0\right)^{-\frac{4}{3}}} \tag{11.3}$$

This determines the value of

$$\rho_0 = \left\{ \frac{L \, (\gamma+1)^{-\frac{1}{3}}}{1.235 \, b_0 \, H} \right\}^{\frac{6}{5}} \left\{ \frac{3}{2} \theta_0 \right\}^{\frac{8}{5}} \tag{11.4}$$

In the case of the closed wind tunnel, ρ_0 from Eq. (11.4) is closely connected to the choking Mach number as can be seen from Fig. 5. From the definition of η in Eq. (3.3) and Bernoulli's equation, one obtains for the local Mach number M

$$M - 1 = \frac{(\gamma+1)^{\frac{2}{3}}}{2} \eta \tag{11.5}$$

From the relation between η and ρ_0 we obtain for the choking Mach number

$$1 - M_c = \frac{(\gamma+1)^{\frac{8}{15}}}{2} \left\{ \frac{L}{1.235 \, b_0 H} \right\}^{\frac{2}{5}} \left(\frac{3\theta_0}{2} \right)^{\frac{8}{15}} \tag{11.6a}$$

or using b_o from Eq. (8.9a) and $\gamma = 1.4$

$$1 - M_c = 1.127 \left\{ \frac{L}{H} \right\}^{\frac{2}{5}} \theta_o^{\frac{8}{15}} \tag{11.6b}$$

For the free-jet one can derive the value of the maximum angular deviation which occurs along the jet boundary in a manner similar to that in the previous paragraph but this is of no practical interest.

The main result will be the determination of the pressure coefficient deviations from the free stream Mach number one wedge caused by restrictions in the flow by a wind tunnel and by a sonic free-jet.

Combining Eqs. (10.5a), (11.1), (11.2), and (11.4) we obtain the following expression for the change of η at a given point x on the body.

$$\Delta \eta = - \frac{b_1}{b_o} (\gamma+1)^{-\frac{2}{5}} \left\{ \frac{L}{1.235 \, b_o \, H} \right\}^{\frac{6}{5}} \left\{ \frac{3 \theta_o}{2} \right\}^{\frac{4}{15}} \frac{\overline{\overline{\varphi_{1\eta}}}}{\varphi_{o\eta\eta}} \tag{11.7a}$$

Or as a function of x/L on the surface of the wedge:

$$\Delta \eta = - \frac{b_1}{b_o} (\gamma+1)^{-\frac{2}{5}} \left\{ \frac{L}{1.235 \, b_o \, H} \right\}^{\frac{6}{5}} \left\{ \frac{3}{2} \theta_o \right\}^{\frac{4}{15}} F\left(\frac{x}{L} \right) \tag{11.7b}$$

where F(x/L) is plotted in Fig. 20 and Fig. 21.

The pressure coefficient C_p is expressed as:

$$C_p = -2(\gamma+1)^{-\frac{1}{3}} \eta \tag{11.8}$$

Combining Eqs. (11.7a) and (11.8)

$$\Delta C_p = 2(\gamma+1)^{-\frac{11}{15}} \left\{ \frac{L}{1.235 \, b_o \, H} \right\}^{\frac{6}{5}} \left\{ \frac{3 \theta_o}{2} \right\}^{\frac{4}{15}} \frac{b_1}{b_o} \frac{\overline{\overline{\varphi_{1\eta}}}}{\varphi_{o\eta\eta}} \tag{11.9a}$$

Or in a more usable form by combining Eqs. (11.7b) and (11.8) and using $\gamma = 1.4$ is obtained

$$\Delta C_p = .910 \left\{ \frac{L}{b_o H} \right\}^{\frac{6}{5}} \theta_o^{\frac{4}{15}} \frac{b_1}{b_o} F\left(\frac{x}{L}\right) \tag{11.9b}$$

Hence we may consider a double wedge of half angle θ_o , of length L in a closed wind tunnel or sonic free-jet of height H and obtain the deviations of the pressure coefficient from Eq. (11.9b). For the solid wall tunnel using the values of b_o and b_1 from Eq. (8.8) can be written as

$$\Delta C_p = 1.802 \, \theta_o^{\frac{4}{15}} \left(\frac{L}{H}\right)^{\frac{6}{5}} F\left(\frac{x}{L}\right) \tag{11.10a}$$

and in a similar manner for the free-jet

$$\Delta C_p = -2.037 \, \theta_o^{\frac{4}{15}} \left(\frac{L}{H}\right)^{\frac{6}{5}} F\left(\frac{x}{L}\right) \tag{11.10b}$$

The pressure coefficient C_p for the double wedge in a free air-flow at Mach number one is given in Ref. 2. We may write it as:

$$C_p = \theta_o^{\frac{2}{3}} \, g\left(\frac{x}{L}\right) \tag{11.11}$$

The function g(x/L) is presented by the solid line in Fig. 22. The total C_p (basic flow plus additional superimposed flow) can be written in the form:

$$C_p = \theta_o^{\frac{2}{3}} \left\{ g\left(\frac{x}{L}\right) + 1.802 \, \theta_o^{-\frac{2}{5}} \left(\frac{L}{H}\right)^{\frac{6}{5}} F\left(\frac{x}{L}\right) \right\} \tag{11.12a}$$

for the closed wind tunnel.

$$C_p = \theta_o^{\frac{2}{3}} \left\{ g\left(\frac{x}{L}\right) - 2.037 \, \theta_o^{-\frac{2}{5}} \left(\frac{L}{H}\right)^{\frac{6}{5}} F\left(\frac{x}{L}\right) \right\} \tag{11.12b}$$

for the sonic free-jet.

It is desirable to discuss briefly the limitations of the analysis. Besides the transonic simplifications which require that the Mach number in the main portions of the flow does not deviate too far from one, the assumption has been made that the value of f_o along which the inner and outer solutions were matched is small. To be specific it must be small in comparison to the values of f which occur along the contour. Along the subsonic contour the smallest value of f which occurs is at C in Figs. 5 and 6. The value is $f_c = \frac{9}{4} \theta_o^2$. By Eq. (11.4) for f_o and the above value for f_c the ratio

$$\frac{f_o}{f_c} = 1.01 \left(\frac{L}{H}\right)^{\frac{6}{5}} \theta_o^{-\frac{2}{5}} \tag{11.13}$$

is obtained for the closed tunnel. The validity of our investigation will increase as this ratio decreases. For the relatively extreme example of an airfoil of a length of 13 per cent of the tunnel height and a thickness ratio of 10 per cent this ratio is found to be 0.219. Results obtained under these conditions can be considered as fairly reliable but not as really accurate.

XII. DISCUSSION OF THE RESULTS

The purpose of the present investigation is to illustrate in a quantitative manner the wall influences in the transonic region. A wedge of 10 per cent thickness ratio and a length of 13 per cent of the closed tunnel height has been considered and the results of Eq. (11.12a) are presented in Fig. 22. The solid line gives the pressure distribution over the wedge in free air with a Mach number of one, while the dotted line gives the distribution in the closed tunnel. It is to be observed that the wall influence is relatively small and this indicates that measurements of this type in a closed choked wind tunnel give a surprisingly good approximation of free flight data.

A comparison of the result of a similar computation for a sonic free-jet of the same height will show that the deviations from free flight conditions are of about the same magnitude but of opposite sign. One would obtain a line slightly underneath the solid line in Fig. 22. Examining the coefficients of the superimposed solution in Eq. (11.12a) and Eq. (11.12b) one notes that the deviations of the pressure distribution are greater in the sonic free-jet than in the choked closed wind tunnel. This indicates that a free-jet tunnel cannot be considered as preferable solely on the basis that the desired free stream Mach number actually occurs upstream of the model. The closed wind tunnel will never attain the free stream Mach number one, but the results obtained are even somewhat better than those obtained in a sonic free-jet. Equation (11.9b) shows the influence of the model dimensions. Naturally the deviation of the pressure distribution will become smaller if the model is smaller in comparison to the tunnel height. The deviation from free air results is proportional to $\left(L/H \right)^{\frac{6}{5}}$. And from Eq. (11.6b)

the deviation of the choking Mach number from one is proportional to

$\left(L/H \right)^{\frac{2}{5}}$. Hence the deviation of the pressure distribution

decreases much faster than the deviation of the choking Mach number from

one with decreasing (L/H). Thus consideration of disturbance to the

pressure distribution based solely on the choking Mach number obtainable

in a wind tunnel is not realistic.

The dependence of the wall influence on the thickness ratio of the

model (in this case on θ_o) is given by $\theta_o^{\frac{4}{15}}$ in Eq. (11.12a). The

absolute deviation of C_p is reduced if θ is decreased, but the

relative accuracy of the measurements becomes smaller, Eqs. (11.12a) and

(11.12b). This behavior is understandable from consideration of transonic

similarity. According to the transonic similarity law, a flow over a

thin body in a wide tunnel will correspond to flow over a thicker body

in a narrower tunnel, if the lengthwise coordinate is kept the same.

These considerations show that the measurements of very slender bodies in

the transonic speed range offer certain difficulties, but extremely

thin bodies are of little interest for practical application from a

structural point of view.

Equation (11.6b) gives the choking Mach number in terms of the

model dimensions. Naturally the validity of this formula is subject to

restriction that the ratio of ρ_o/ρ_c is small, Eq. (11.13). It shows that

the choking Mach number is not directly determined by the one dimensional

flow area ratio considerations, otherwise the powers of $\frac{L}{H}$ and θ_o would be $\frac{1}{2}$.

Although the present results indicate that measurements in a closed

wind tunnel may be quite valuable in the transonic region, one should be

careful not to generalize this result too quickly. The result has been

found for two dimensional flow and while investigations of axial

symmetric transonic flow show the behavior is similar to planar flows there are also marked differences (Ref. 7).

REFERENCES

1. Guderley, Gottfried: "Two Dimensional Flow Patterns with a Free Stream Mach Number Close to One", Wright Field Report No. 6343, May 1951.

2. Guderley, Gottfried and Yoshihara, Hideo: "The Flow Over a Wedge Profile at Mach Number One", Wright Field Report No. 5783, July 1949.

3. Tricomi, F.: "On Linear Partial Differential Equations of the Second Order of Mixed Type", Brown University Translation A9-T-26, (To be printed as a Central Air Documents Office Translation in the near future). Original source: Atti della R. Accademia Nazionale dei Lincei 1923. Serie Quinta, Memorie della Classe di Scienze Fisiche, Matematiche e Naturali, Volume XIV, p. 134.

4. The Computation Laboratory, Harvard University, Cambridge, Massachusetts: "Flow Patterns with a Free Stream Mach Number Close to One", Report No. 16.

5. Guderley, Gottfried: "Singularities at the Sonic Velocity", Wright Field Report F-TR-1171-ND.

6. Hamel, Georg: "Integralgleichungen", Berlin, Springer Verlag, 1937.

7. Guderley, Gottfried: "Axial-Symmetric Flow Patterns at a Free Stream Mach Number Close to One", Wright Field Report No. 6285, October 1950.

APPENDIX Ia

ON THE FUNCTIONS $G(\xi, \lambda)$

The material in this appendix is discussed in detail in Refs. 1 and 5.

The basic equation for the stream function derived from the application of the transonic similarity law is given by:

$$\psi_{\eta\eta} - \eta\,\psi_{\theta\theta} = 0 \tag{Ia.1}$$

The following change of independent variables is introduced:

$$\xi = \eta \Big/ \left(\tfrac{3}{2}\theta\right)^{\frac{2}{3}} \tag{Ia.2}$$

and

$$\rho = -\eta^3 + \left(\tfrac{3}{2}\theta\right)^2 \tag{Ia.3}$$

With this change of variables, Eq. (Ia.1) becomes

$$\frac{(1-\xi^3)^2}{\xi}\,\psi_{\xi\xi} - \tfrac{5}{2}\xi\left(1-\xi^3\right)\psi_\xi + \tfrac{1}{16}\psi = 9\rho^2\psi_{\rho\rho} + \tfrac{21}{2}\rho\,\psi_\rho + \tfrac{1}{16}\psi \tag{Ia.4}$$

Introducing the product hypothesis

$$\psi = g(\rho)\,G(\xi) \tag{Ia.5}$$

into Eq. (Ia.4), the following equation for $G(\xi)$ is obtained:

$$\frac{(1-\xi^3)^2}{\xi}\frac{d^2 G(\xi)}{d\xi^2} - \tfrac{5}{2}\xi\left(1-\xi^3\right)\frac{dG(\xi)}{d\xi} + \left(-\lambda + \tfrac{1}{16}\right)G(\xi) = 0 \tag{Ia.6}$$

λ is a constant which is introduced in the separation of variables. The function $G(\xi)$ will also depend on the value of λ, hence the function will be expressed as $G(\xi, \lambda)$.

The equation for $G(\xi, \lambda)$, Eq. (Ia.6), is closely connected to the hypergeometric differential equation. Equation (Ia.6) will be transformed by the introduction of the following change of variables

$$\zeta = \xi^{-3} \tag{Ia.7a}$$

$$\eta = -\tfrac{1}{4} \pm \sqrt{\lambda} \tag{Ia.7b}$$

$$G(\xi, \lambda) = |\zeta - 1|^{-\frac{\eta}{3}} f(\zeta, \eta) \tag{Ia.7c}$$

With these the following equation is obtained:

$$\zeta(\zeta-1)f'' + \left(-\tfrac{1}{2} + \left[\tfrac{4}{3} - \tfrac{2}{3}\eta\right]\zeta\right)f' + \frac{\eta(\eta-1)}{9}f = 0 \tag{Ia.8}$$

This equation has three regular singular points and is a hypergeometric differential equation. As the properties of this differential equation are well known, the solutions can be easily constructed. The representations of the solution for various regions of convergence of this equation as tabulated in Section III of Ref. 5, which are Kummer's solutions specialized to the case of the above differential equation, Eq. (Ia.8), are presented with the equations numbered as in Ref. 5:

$$u_1 = \left(\tfrac{1}{\zeta}\right)^{-\frac{\eta}{3}} F\left(-\tfrac{\eta}{3}, \frac{-2\eta+3}{6}, \tfrac{2}{3}; \tfrac{1}{\zeta}\right) \qquad /\!5\!/\text{-}(3,20a)$$

$$v_1 = \left(\tfrac{1}{\zeta}\right)^{\frac{1-\eta}{3}} F\left(\frac{1-\eta}{3}, \frac{-2\eta+5}{6}, \tfrac{4}{3}; \tfrac{1}{\zeta}\right) \qquad /\!5\!/\text{-}(3,20b)$$

$$u_1 = \left(\tfrac{1}{\zeta}\right)^{-\frac{\eta}{3}} \left(\frac{\zeta-1}{\zeta}\right)^{\frac{4\eta+1}{6}} F\left(\frac{2\eta+1}{6}, \frac{\eta+2}{3}, \tfrac{2}{3}; \tfrac{1}{\zeta}\right) \qquad /\!5\!/\text{-}(3,20c)$$

$$v_1 = \left(\tfrac{1}{\zeta}\right)^{\frac{1-\eta}{3}} \left(\frac{\zeta-1}{\zeta}\right)^{\frac{4\eta+1}{6}} F\left(\frac{2\eta+3}{6}, \frac{\eta+3}{3}, \tfrac{4}{3}; \tfrac{1}{\zeta}\right) \qquad /\!5\!/\text{-}(3,20d)$$

where the region of convergence is given by: $|\zeta| > 1$

- - - - - - - - - -

$$\bar{u}_2 = \left(\frac{-1}{\zeta-1}\right)^{-\frac{\eta}{3}} \cdot F\left(-\frac{\eta}{3}, \frac{2\eta+1}{6}, \frac{1}{2}; \frac{\zeta}{\zeta-1}\right)$$

$\quad$ [5]-(3,21a)

$$\bar{v}_2 = \left(\frac{\zeta}{\zeta-1}\right)^{\frac{1}{2}}\left(\frac{-1}{\zeta-1}\right)^{-\frac{\eta}{3}} \cdot F\left(\frac{-2\eta+3}{6}, \frac{\eta+2}{3}, \frac{3}{2}; \frac{\zeta}{\zeta-1}\right)$$

$\quad$ [5]-(3,21b)

$$\bar{u}_2 = \left(\frac{-1}{\zeta-1}\right)^{\frac{1-\eta}{3}} \cdot F\left(\frac{-\eta+1}{3}, \frac{2\eta+3}{6}, \frac{1}{2}; \frac{\zeta}{\zeta-1}\right)$$

$\quad$ [5]-(3,21c)

$$\bar{v}_2 = \left(\frac{\zeta}{\zeta-1}\right)^{\frac{1}{2}}\left(\frac{-1}{\zeta-1}\right)^{\frac{1-\eta}{3}} \cdot F\left(\frac{-2\eta+5}{6}, \frac{\eta+3}{3}, \frac{3}{2}; \frac{\zeta}{\zeta-1}\right)$$

$\quad$ [5]-(3,21d)

where the region of convergence is given by: $Rl\ \zeta < \frac{1}{2}$

- - - - - - - - - -

$$u_3 = F\left(-\frac{\eta}{3}, \frac{-\eta+1}{3}, \frac{-4\eta+5}{6}; 1-\zeta\right)$$

$\quad$ [5]-(3,22a)

$$v_3 = (1-\zeta)^{\frac{4\eta+1}{6}} F\left(\frac{2\eta+1}{6}, \frac{2\eta+3}{6}, \frac{4\eta+7}{6}; 1-\zeta\right)$$

$\quad$ [5]-(3,22b)

$$u_3 = \zeta^{\frac{1}{2}} F\left(\frac{-2\eta+3}{6}, \frac{-2\eta+5}{6}, \frac{-4\eta+5}{6}; 1-\zeta\right)$$

$\quad$ [5]-(3,22c)

$$v_3 = (1-\zeta)^{\frac{4\eta+1}{6}} \zeta^{\frac{1}{2}} F\left(\frac{\eta+2}{3}, \frac{\eta+3}{3}, \frac{4\eta+7}{6}; 1-\zeta\right)$$

$\quad$ [5]-(3,22d)

where the region of convergence is given by: $|\zeta-1| < 1$

- - - - - - - - - -

$$\bar{u}_1 = \left(\frac{1}{1-\zeta}\right)^{-\frac{2}{3}} \cdot F\left(-\frac{2\eta}{3},\ \frac{2\eta+1}{6},\ \frac{2}{3};\ \frac{1}{1-\zeta}\right) \qquad \boxed{5}\text{-(3,23a)}$$

$$\bar{v}_1 = \left(\frac{1}{1-\zeta}\right)^{\frac{1-\eta}{3}} \cdot F\left(\frac{-\eta+1}{3},\ \frac{2\eta+3}{6},\ \frac{4}{3};\ \frac{1}{1-\zeta}\right) \qquad \boxed{5}\text{-(3,23b)}$$

$$\bar{u}_1 = \left(\frac{1}{1-\zeta}\right)^{-\frac{2}{3}} \left(\frac{\zeta}{\zeta-1}\right)^{\frac{1}{2}} \cdot F\left(\frac{-2\eta+3}{6},\ \frac{-\eta+2}{3},\ \frac{2}{3};\ \frac{1}{1-\zeta}\right) \qquad \boxed{5}\text{-(3,23c)}$$

$$\bar{v}_1 = \left(\frac{1}{1-\zeta}\right)^{\frac{1-\eta}{3}} \left(\frac{\zeta}{\zeta-1}\right)^{\frac{1}{2}} \cdot F\left(\frac{-2\eta+5}{6},\ \frac{\eta+3}{3},\ \frac{4}{3};\ \frac{1}{1-\zeta}\right) \qquad \boxed{5}\text{-(3,23d)}$$

where the region of convergence is given by: $|\zeta - 1| > 1$

- - - - - - - - - -

$$\bar{u}_3 = \left(\frac{1}{\zeta}\right)^{-\frac{2}{3}} \cdot F\left(-\frac{2\eta}{3},\ \frac{-2\eta+3}{6},\ \frac{-4\eta+5}{6};\ \frac{\zeta-1}{\zeta}\right) \qquad \boxed{5}\text{-(3,24a)}$$

$$\bar{v}_3 = \left(\frac{\zeta-1}{\zeta}\right)^{\frac{4\eta+1}{6}} \left(\frac{1}{\zeta}\right)^{-\frac{2}{3}} \cdot F\left(\frac{2\eta+1}{6},\ \frac{\eta+2}{3},\ \frac{4\eta+7}{6};\ \frac{\zeta-1}{\zeta}\right) \qquad \boxed{5}\text{-(3,24b)}$$

$$\bar{u}_3 = \left(\frac{1}{\zeta}\right)^{\frac{1-\eta}{3}} \cdot F\left(\frac{-\eta+1}{3},\ \frac{-2\eta+5}{6},\ \frac{-4\eta+5}{6};\ \frac{\zeta-1}{\zeta}\right) \qquad \boxed{5}\text{-(3,24c)}$$

$$\bar{v}_3 = \left(\frac{\zeta-1}{\zeta}\right)^{\frac{4\eta+1}{6}} \left(\frac{1}{\zeta}\right)^{\frac{1-\eta}{3}} \cdot F\left(\frac{2\eta+3}{6},\ \frac{\eta+3}{3},\ \frac{4\eta+7}{6};\ \frac{\zeta-1}{\zeta}\right) \qquad \boxed{5}\text{-(3,24d)}$$

where the region of convergence is given by: $\mathcal{R}l\,\zeta > 1/2$

- - - - - - - - - -

$$u_2 = F\left(-\frac{\eta}{3}, \frac{-\eta+1}{3}, \frac{1}{2}; \zeta\right) \qquad \boxed{5}\text{-}(3,25a)$$

$$v_2 = \zeta^{\frac{1}{2}} F\left(\frac{-2\eta+3}{6}, \frac{-2\eta+5}{6}, \frac{3}{2}; \zeta\right) \qquad \boxed{5}\text{-}(3,25b)$$

$$u_2 = (1-\zeta)^{\frac{4\eta+1}{6}} F\left(\frac{2\eta+1}{6}, \frac{2\eta+3}{6}, \frac{1}{2}; \zeta\right) \qquad \boxed{5}\text{-}(3,25c)$$

$$v_2 = \zeta^{\frac{1}{2}}(1-\zeta)^{\frac{4\eta+1}{6}} F\left(\frac{\eta+2}{3}, \frac{\eta+3}{3}, \frac{3}{2}; \zeta\right) \qquad \boxed{5}\text{-}(3,25d)$$

where the region of convergence is given by: $\quad |\zeta| < 1$

- - - - - - - - - -

The condition that G(ξ, λ) = 0 for ξ = $-\infty$ is transformed into the condition f(ζ, η) = 0 for ζ = 0.

A function f(ζ, η) is represented by a linear combination of the functions $\overline{u}_2$ and $\overline{v}_2$ in the vicinity of ζ = 0. From inspection of $\overline{u}_2$ and $\overline{v}_2$ in Eq. $\boxed{5}$-(3,21a) and Eq. $\boxed{5}$-(3,21b), it is seen that $\overline{u}_2$ = 1 and $\overline{v}_2$ = 0 at the origin ζ = 0. So from the above condition at ζ = 0, the function f(ζ, η) will be represented by $\overline{v}_2$. Denote this function f(ζ, η) which is needed for the representation of G(ξ, λ) in Eq. (Ia.7c) by fIII(ζ, η). From fIII(ζ, η) discussed above together with the above tabulation of formulae given in Ref. 5 Section IIIf connecting u_i and v_i and Eq. (Ia.7c) we obtain formulae for $\mathcal{G}$(ξ, λ). These are given in Ref. 1 and are tabulated below with numbering utilized in Ref. 1.

$$G(\xi,\lambda) = \left(\frac{1}{1-\xi^3}\right)^{\frac{1}{2}} F\left(-\frac{\sqrt{\lambda}}{3}+\frac{7}{12}, \frac{\sqrt{\lambda}}{3}+\frac{7}{12}, \frac{3}{2}; \frac{1}{1-\xi^3}\right) \qquad \boxed{I}\text{-18a}$$

valid from $\xi = -\infty$ to $\xi = 0$

$$G(\xi,\lambda) = \frac{\frac{3}{2}\cdot\Gamma\left(\frac{4}{3}\right)\cdot\Gamma\left(\frac{1}{2}\right)}{\Gamma\left(\frac{\sqrt{\lambda}}{3}+\frac{11}{12}\right)\Gamma\left(-\frac{\sqrt{\lambda}}{3}+\frac{11}{12}\right)} F\left(-\frac{\sqrt{\lambda}}{3}+\frac{1}{12}, \frac{\sqrt{\lambda}}{3}+\frac{1}{12}, \frac{2}{3}; \frac{\xi^3}{\xi^3-1}\right) \qquad \boxed{I}\text{-18b}$$

$$-\frac{\frac{3}{2}\Gamma\left(\frac{2}{3}\right)\Gamma\left(\frac{1}{2}\right)}{\Gamma\left(\frac{\sqrt{\lambda}}{3}+\frac{7}{12}\right)\Gamma\left(-\frac{\sqrt{\lambda}}{3}+\frac{7}{12}\right)}\frac{\xi}{(\xi^3-1)^{\frac{1}{3}}} F\left(-\frac{\sqrt{\lambda}}{3}+\frac{5}{12}, \frac{\sqrt{\lambda}}{3}+\frac{5}{12}, \frac{4}{3}; \frac{\xi^3}{\xi^3-1}\right)$$

valid from $\xi = -\infty$ to $\xi = 2^{-\frac{1}{3}}$

- - - - - - - -

$$G(\xi,\lambda) = \frac{\frac{3}{2}\Gamma\left(\frac{4}{3}\right)\Gamma\left(\frac{1}{2}\right)}{\Gamma\left(\frac{\sqrt{\lambda}}{3}+\frac{11}{12}\right)\cdot\Gamma\left(-\frac{\sqrt{\lambda}}{3}+\frac{11}{12}\right)}\left(1-\xi^3\right)^{\frac{1}{12}-\frac{\sqrt{\lambda}}{3}}\cdot F\left(-\frac{\sqrt{\lambda}}{3}+\frac{1}{12}, -\frac{\sqrt{\lambda}}{3}+\frac{7}{12}, \frac{2}{3}; \xi^3\right) \qquad \boxed{I}\text{-18c}$$

$$+\frac{\frac{3}{2}\Gamma\left(\frac{2}{3}\right)\cdot\Gamma\left(\frac{1}{2}\right)}{\Gamma\left(\frac{\sqrt{\lambda}}{3}+\frac{7}{12}\right)\cdot\Gamma\left(\frac{\sqrt{\lambda}}{3}+\frac{1}{12}\right)}\left(1-\xi^3\right)^{\frac{1}{12}-\frac{\sqrt{\lambda}}{3}}\cdot\xi\cdot F\left(-\frac{\sqrt{\lambda}}{3}+\frac{5}{12}, -\frac{\sqrt{\lambda}}{3}+\frac{11}{12}, \frac{4}{3}; \xi^3\right)$$

valid from $\xi = -1$ to $\xi = 1$

- - - - - - - - -

$$G(\xi,\lambda) = \Gamma\left(\frac{1}{2}\right)\left\{ \frac{\Gamma\left(\frac{2}{3}\sqrt{\lambda}\right)\sin\pi\left(\frac{\sqrt{\lambda}}{3}+\frac{1}{4}\right)}{\Gamma\left(\frac{\sqrt{\lambda}}{3}+\frac{11}{12}\right)\cdot\Gamma\left(\frac{\sqrt{\lambda}}{3}+\frac{7}{12}\right)}\left(1-\xi^3\right)^{\frac{1}{12}-\frac{\sqrt{\lambda}}{3}}\cdot F\left(-\frac{\sqrt{\lambda}}{3}+\frac{1}{12}, -\frac{\sqrt{\lambda}}{3}+\frac{7}{12}, -\frac{2}{3}\sqrt{\lambda}+1; 1-\xi^3\right)\right.$$

$$\left. +\frac{\Gamma\left(-\frac{2}{3}\sqrt{\lambda}\right)\sin\pi\left(-\frac{\sqrt{\lambda}}{3}+\frac{1}{4}\right)}{\Gamma\left(-\frac{\sqrt{\lambda}}{3}+\frac{11}{12}\right)\cdot\Gamma\left(-\frac{\sqrt{\lambda}}{3}+\frac{7}{12}\right)}\left(1-\xi^3\right)^{\frac{1}{12}+\frac{\sqrt{\lambda}}{3}}\cdot F\left(\frac{\sqrt{\lambda}}{3}+\frac{1}{12}, \frac{\sqrt{\lambda}}{3}+\frac{7}{12}, \frac{2}{3}\sqrt{\lambda}+1; 1-\xi^3\right)\right\} \quad \boxed{I}\text{-18d}$$

valid from $\xi = 0$ to $\xi = 2^{1/3}$

- - - - - - - - -

The above formulae for $G(\xi, \lambda)$ are solutions to the differential equation, Eq.(Ia.6), in the indicated regions of validity. The formulae for $G(\xi, \lambda)$ also satisfies the condition $G(\xi, \lambda) = 0$ for $\xi = -\infty$ as is required by the boundary value prescription on the stream function in the special cases under consideration.

APPENDIX I

ON THE REPRESENTATION OF THE OUTER SOLUTION

Assume that

$$\overline{\psi}_h = \psi_{II_h} + \widetilde{\psi}_h \tag{I.1}$$

are expressions which fulfill the boundary conditions $\psi = 0$ along the entire line OABBCD in Fig. 8. Here ψ_{II_h} is the solution defined in Eq. (5.3b) and $\widetilde{\psi}_h$ is a function which fulfills the conditions of Tricomi's existence and uniqueness proof. Now consider ψ a function that satisfies the Tricomi equation outside of a line $\rho = \rho_o$ and furthermore fulfills the boundary condition $\psi = 0$ along the boundary. We shall show that ψ can be represented by a superposition of the functions $\overline{\psi}_h$. For this purpose it is assumed that a sequence of solutions of Tricomi's equation will converge if the sequence of the boundary values prescribed form a convergent sequence. In other words it is assumed that the solution of Tricomi's problem depends continuously upon the prescribed boundary values.

Inside the region AB'CD'E in Fig. 8 bounded by $\rho = \rho_o$, $\rho = \rho_c$, $\xi = -\infty$, and $\xi = C_2$ the expression can be developed because of the completeness of the system of eigen functions (This development is discussed in detail in Appendix I of Ref. 1) in the form

$$\psi = \sum_h C_{I_h} \psi_{I_h} + \sum_h C_{II_h} \psi_{II_h} + \sum_h C_{III_h} \psi_{III_h} + \sum_h C_{IV_h} \psi_{IV_h} \tag{I.2}$$

The expression $\sum_h C_{II_h} \psi_{II_h}$ will converge for $\rho > \rho_o$. In particular it will converge along the boundary B'CD, and along the θ axis it is zero since all of the expressions ψ_{II_h} are zero along this line.

Now form solutions of the Tricomi problem which have the boundary values ψ along the boundary OAB'CD given by the partial sums of $\sum_{h} C_{\amalg_h} \psi_{\amalg_h}$. The sequence of the boundary values will converge and therefore also the sequence of the Tricomi solutions according to the theorem assumed above. Now because of the definition of $\widetilde{\psi_h}$ the sequence of solutions of the Tricomi problem just mentioned is identical term by term with the sequence of the partial sums of the series $\sum C_{\amalg_h} \overline{\psi_h}$. Hence it follows that this last series converges in the entire region and therefore the series of the expressions

$$\sum_{h} C_{\amalg_h} \overline{\psi_h} = \sum_{h} C_{\amalg_h} \left\{ \psi_{\amalg_h} + \widetilde{\psi_h} \right\} \qquad (I.3)$$

will converge.

The difference of the two expressions Eq. (I.2) and Eq. (I.3) represents a function that does not contain a term $\psi_{\amalg_h}$ and has the prescription of $\psi = 0$ along the boundary, hence by uniqueness proof given Paragraph 5, Section III of Ref. 1 this function is identically zero. Thus Eq. I.3 is a representation of the original function ψ .

APPENDIX II

DETERMINATION OF THE UNKNOWN COEFFICIENTS

A. Free-Jet Case

The representation of the solution in the inner region ($\rho < \rho_o$) of Fig. 6 is

$$\psi = \sum_{h=0} a_h \left(\frac{\rho}{\rho_o} \right)^{\frac{5}{6}+h} G \left\{ \xi, \left(\frac{11}{4} + 3h \right)^2 \right\} + H(\xi) \qquad (II.1)$$

H(ξ) is a solution of the differential equation for G(ξ, λ) for λ = 1/16 which reduces then to

$$\frac{d}{d\xi} \left[(1 - \xi^3)^{\frac{5}{6}} \frac{dH(\xi)}{d\xi} \right] = 0 \qquad (II.2)$$

It satisfies the following boundary conditions

$$H(-\infty) = 0 \qquad (II.3a)$$

$$H(0) = 1 \qquad (II.3b)$$

The representation of the solution in the outer region ($\rho > \rho_o$) of Fig 6 is given by

$$\psi = \sum_{h=0} b_h \left(\frac{\rho}{\rho_o} \right)^{-\frac{5}{6}-h} G \left\{ \xi, \left(\frac{9}{4} + 3h \right)^2 \right\} \qquad (II.4)$$

The two representations and their normal derivatives are matched along the curve $\rho = \rho_o$ to obtain the following equations

$$H(\xi) + \sum_{h=0} a_h G \left\{ \xi, \left(\frac{11}{4} + 3h \right)^2 \right\} = \sum_{h=0} b_h G \left\{ \xi, \left(\frac{9}{4} + 3h \right)^2 \right\} \qquad (II.5a)$$

$$\sum_{h=0} \left(\frac{5}{6} + a_h \right) G \left\{ \xi, \left(\frac{11}{4} + 3h \right)^2 \right\} = \sum_{h=0} \left(-\frac{5}{6} - h \right) b_h G \left\{ \xi, \left(\frac{9}{4} + 3h \right)^2 \right\} \qquad (II.5b)$$

We multiply these equations with $\dfrac{\xi\, G\left(\xi,\left(\frac{11}{4}+3h\right)^2\right)}{(1-\xi^3)^{\frac{7}{6}}}$ and integrate from

$-\infty$ to 0. The functions $G(\xi, \lambda_h)$ are orthogonal to each other, therefore the mth equation will contain only one term a_m. One obtains

$$\int_{-\infty}^{0} H(\xi)\, \frac{G\left\{\xi,\left(\frac{11}{4}+3m\right)^2\right\}\,\xi}{(1-\xi^3)^{\frac{7}{6}}}\, d\xi \;+\; a_m \int_{-\infty}^{0} \frac{\xi\, d\xi}{(1-\xi^3)^{\frac{7}{6}}}\left[G\left\{\xi,\left(\frac{11}{4}+3m\right)^2\right\}\right]^2$$

$$= \sum_{h} b_h \int_{-\infty}^{0} G\left\{\xi,\left(\frac{9}{4}+3h\right)^2\right\} G\left\{\xi,\left(\frac{11}{4}+3m\right)^2\right\} \frac{\xi}{(1-\xi^3)^{\frac{7}{6}}}\, d\xi \tag{II.6a}$$

and

$$\left(\frac{5}{6}+m\right) a_m \int_{-\infty}^{0} \frac{\xi}{(1-\xi^3)^{\frac{7}{6}}}\left[G\left\{\xi,\left(\frac{11}{4}+3m\right)^2\right\}\right]^2 d\xi$$

$$= \sum_{h=0}\left(-\frac{5}{6}-h\right) b_h \int_{-\infty}^{0} G\left\{\xi,\left(\frac{9}{4}+3h\right)^2\right\} G\left\{\xi,\left(\frac{11}{4}+3m\right)^2\right\} \frac{\xi}{(1-\xi^3)^{\frac{7}{6}}}\, d\xi \tag{II.6b}$$

Combining the mth equations of the systems of Eq. (II.6a) and (II.6b) one obtains a system of equations for the coefficients b_h.

$$\int_{-\infty}^{0} H(\xi)\, G\left\{\xi,\left(\frac{11}{4}+3m\right)^2\right\} \frac{\xi}{(1-\xi^3)^{\frac{7}{6}}}\, d\xi$$

$$= \sum \left[\frac{1+\frac{5}{6}+h}{\frac{5}{6}+m}\right] b_h \int_{-\infty}^{0} G\left\{\xi,\left(\frac{9}{4}+3h\right)^2\right\} G\left\{\xi,\left(\frac{11}{4}+3m\right)^2\right\} \frac{\xi}{(1-\xi^3)^{\frac{7}{6}}}\, d\xi \tag{II.7}$$

The integrals which occur here can be evaluated in a closed form. Let

$$D_m = \int_{-\infty}^{0} H(\xi)\, G\left\{\xi, \left(\tfrac{11}{4}+3m\right)^2\right\} \frac{\xi}{(1-\xi^3)^{\frac{7}{6}}}\, d\xi \tag{II.8}$$

From the differential equation for $G(\xi, \lambda)$ in the self adjoint

form Eq. (4.14), one obtains

$$\frac{d\left[(1-\xi^3)^{\frac{5}{6}} \frac{dG(\xi,\lambda_h)}{d\xi}\right]}{d\xi} = \left(\lambda_h - \tfrac{1}{16}\right) \frac{\xi}{(1-\xi^3)^{\frac{7}{6}}}\, G(\xi, \lambda_h) \tag{II.9}$$

Inserting this into Eq. (II.8) one obtains

$$D_m = \frac{1}{\left(\tfrac{11}{4}+3m\right)^2 - \tfrac{1}{16}} \int_{-\infty}^{0} H(\xi) \frac{d}{d\xi}\left[(1-\xi^3)^{\frac{5}{6}} \frac{dG\left\{\xi, \left(\tfrac{11}{4}+3m\right)^2\right\}}{d\xi}\right] d\xi \tag{II.10}$$

An integration by parts yeilds

$$D_m = \left[\frac{1}{\left(\tfrac{11}{4}+3m\right)^2 - \tfrac{1}{16}}\right] \left\{ H(\xi)(1-\xi^3)^{\frac{5}{6}} \frac{dG\left\{\xi, \left(\tfrac{11}{4}+3m\right)^2\right\}}{d\xi} \right\} \Bigg|_{-\infty}^{0}$$

$$- \int_{-\infty}^{0} \frac{dH\left[(1-\xi^3)^{\frac{5}{6}}\right]}{d\xi} \frac{dG\left\{\xi, \left(\tfrac{11}{4}+3m\right)^2\right\}}{d\xi}\, d\xi \tag{II.11}$$

Because of Eq. (II.2) the last integral vanishes and with the boundary

conditions on $H(\xi)$ one obtains

$$D_m = \frac{1}{\left(\tfrac{11}{4}+3m\right)^2 - \tfrac{1}{16}} \frac{dG\left\{\xi, \left(\tfrac{11}{4}+3m\right)^2\right\}}{d\xi} \Bigg|_{-\infty}^{0} \tag{II.12}$$

Quite similarily one finds that

$$E_{mh} = \int_{-\infty}^{0} G\left\{\xi, \left(\tfrac{9}{4}+3h\right)^2\right\} G\left\{\xi, \left(\tfrac{11}{4}+3m\right)^2\right\} \frac{\xi}{(1-\xi^3)^{\frac{7}{6}}}\, d\xi \tag{II.13}$$

can be expressed as

$$E_{mh} = \frac{G\left\{\xi, \left(\tfrac{9}{4}+3h\right)^2\right\} G'\left\{\xi, \left(\tfrac{11}{4}+3m\right)^2\right\}}{\left(\tfrac{11}{4}+3m\right)^2 - \left(\tfrac{9}{4}+3h\right)^2} \Bigg|_{\xi=0} \tag{II.14}$$

From the representations from $G(\xi, \lambda_h)$ in terms of hyper-geometric functions (Eq. 18 in Ref. 1) one finds that

$$G'\left\{\xi, \left(\tfrac{11}{4}+3m\right)^2\right\} = -(-1)^m \frac{3}{2} \frac{\tfrac{1}{3}\cdot\tfrac{4}{3}\cdots\left(\tfrac{1}{3}+m\right)}{\tfrac{1}{2}\cdot\tfrac{3}{2}\cdots\left(\tfrac{1}{2}+m\right)} \qquad \text{(II.15a)}$$

$$G\left\{\xi, \left(\tfrac{9}{4}+3h\right)^2\right\} = -(-1)^h \frac{3\cdot2^{\tfrac{1}{3}}}{2} \frac{\left(-\tfrac{1}{6}\right)\cdots\left(-\tfrac{1}{6}+h\right)}{\left(\tfrac{2}{3}\right)\cdots\left(\tfrac{2}{3}+h\right)} \qquad \text{(II.15b)}$$

With these expressions Eq. (II.12) and Eq. (II.14) can be computed. The E_{mh} represent the elements of the matric of the linear system of equations for the coefficients b_h, the D_m the negative values of the right hand side. It is possible to approximate this infinite system by a finite number of equations as the above system satisfies the condition of E. Schmidt (Cf. Ref. 5). Using a system of seven equations the first two coefficients b_h are

$$b_o = .395 \qquad \text{(II.16a)}$$

$$b_1 = .290 \qquad \text{(II.16b)}$$

B. Solid Wall Tunnel Case

The representation of the solution in the outer region ($\rho > \rho_o$) of Fig. 5 is the same as in the free-jet case Eq. (II.4). The representation of the solution in the inner region is given by:

$$\psi = \sum a_h \left(\frac{\rho}{\rho_o}\right)^{\tfrac{2}{3}+h} G\left\{\xi, \left(\tfrac{9}{4}+3h\right)^2\right\} + \sum C_h \left(\frac{\rho}{\rho_o}\right)^{-\tfrac{1}{2}} G\left\{\xi, \left(\tfrac{9}{4}+3h\right)^2\right\} \cos\left(\tfrac{2h}{3}\log\frac{\rho}{\rho_o}\right)$$

$$+ \sum d_h \left(\frac{\rho}{\rho_o}\right)^{-\tfrac{1}{2}} G\left\{\xi, \left(\tfrac{9}{4}+3h\right)^2\right\} \sin\left(\tfrac{2h}{3}\log\frac{\rho}{\rho_o}\right) + H(\xi) \qquad \text{(II.17)}$$

Where $H(\xi)$ is defined by Eq. (II.2) and satisfies the following boundary conditions:

$$H(-\infty) = 1 \quad \text{and} \quad H(1) = 0 \tag{II.18}$$

The matching process along the boundary curve $\rho = \rho_o$ is again carried out. Since the inner and outer representations have the same eigen values $\left(\lambda_h = \left(\frac{9}{4} + h\right)^2\right)$ and form a system of orthogonal functions the results are greatly simplified. The resulting equations from the matching process are multiplied by $\frac{\xi}{(1-\xi^3)^{\frac{1}{2}}} G\left\{\xi, \left(\frac{9}{4} + 3h\right)^2\right\}$ and integrated from $-\infty$ to 1. Introducing

$$C_h = \int_{-\infty}^{1} \frac{\xi}{(1-\xi^3)^{\frac{1}{2}}} \left[G\left\{\xi, \left(\frac{9}{4} + 3h\right)^2\right\}\right]^2 d\xi \tag{II.19}$$

$$D_h = \int_{-\infty}^{1} H(\xi) \, G\left\{\xi, \left(\frac{9}{4} + 3h\right)^2\right\} \frac{\xi}{(1-\xi^3)^{\frac{1}{2}}} \, d\xi \tag{II.20}$$

the following relations are obtained

$$D_h + a_h \, C_h = b_h \, C_h \tag{II.21}$$

$$\left(\frac{2}{3} + h\right) a_h \, C_h = \left(-\frac{5}{6} - h\right) b_h \, C_h \tag{II.22}$$

Hence

$$b_h = \frac{D_h}{C_h} \frac{h + \frac{2}{3}}{2h + \frac{3}{2}} \tag{II.23}$$

The integral D_h is determined in a manner similar to the evaluation of the integral D_m, Eq. (II.8), with the result

$$D_h = \frac{-\frac{3}{2}}{\left(\frac{9}{4} + 3h\right)^2 - \frac{1}{16}} \tag{II.24}$$

The evaluation of the integral C_h is carried out on the basis of Appendix IV of Ref. 1 with the result

$$C_h = \frac{\pi\sqrt{3}\cdot 1}{\left(\frac{3}{2}+2h\right)2} \; \frac{-\frac{1}{6}\cdot\frac{5}{6}\cdots\left(-\frac{1}{6}+h\right)}{\frac{2}{3}\cdot\frac{5}{3}\cdots\left(\frac{2}{3}+h\right)} \; \frac{\frac{1}{6}\cdots\left(\frac{1}{6}+h\right)}{\frac{1}{3}\cdots\left(\frac{1}{3}+h\right)} \qquad \text{(II.25)}$$

And thus in a direct manner without having to solve a system of linear equations one obtains the first two coefficients

$$b_0 \;=\; .586 \qquad\qquad\qquad \text{(II.26a)}$$

$$b_1 \;=\; .611 \qquad\qquad\qquad \text{(II.26b)}$$

APPENDIX III

DETAILS OF THE DETERMINATION OF THE PARTICULAR SOLTUION $\overline{\overline{\psi}}_I$

The problem under consideration is the determination of the solution to the differential equation of Tricomi, Eq. (3.5), with the boundary conditions of ψ = 0 along the line OABBCD of Fig. 8 and with a singularity at the origin given by

$$\psi_{II_I} = \rho^{-\frac{4}{6}} \, G \left\{ \xi, \left(\frac{9}{4}+3\right)^2 \right\} \tag{III.1}$$

The function $G \left\{ \xi, (9/4 + 3)^2 \right\}$ is tabulated in Ref. 4 for the subsonic region. In the supersonic region some unpublished results of the same source were utilized; in the vicinity of the critical region near ξ = 1 they were supplemented by some hand computations.

The above problem is analogous to that of the flow over a wedge at Mach number one in Ref. 2, the difference being that in Ref. 2 the singularity at the origin is given by ψ_{II_o} .

The boundary conditions along θ = 0 and $\theta = \theta_o$ will be fulfilled by an image system of the singularities given in Eq. (III.1) spaced at intervals of $2\theta_o$ along the θ axis. Since the expression, Eq. (III.1) is antisymmetric with respect to the θ = 0 axis all of the singularities will occur with the same sign, Fig. 9. Denoting the portion of the stream function obtained by this image system as $\overline{\psi}_I^{(i)}$ one has

$$\overline{\psi}_I^{(i)} = \sum_{m=-\infty}^{\infty} \rho_m^{-\frac{4}{6}} \, G \left\{ \xi_m, \left(\frac{9}{4}+3\right)^2 \right\} \tag{III.2}$$

where

$$f_m = -\eta^3 + \left\{ \tfrac{3}{2} (\theta - 2m\theta_0) \right\}^2 \qquad (III.3)$$

and

$$\xi_m = \frac{\eta}{\left\{ \tfrac{3}{2} (\theta - 2m\theta_0) \right\}^{\frac{2}{3}}} \qquad (III.4)$$

If $\theta - 2m\theta_0$ is negative then the value of Ref. 4 for the
$G\left\{ \xi , (9/4 + 3)^2 \right\}$ must be multiplied by minus one.

For the fulfillment of the boundary conditions along the shoulder
of the wedge (Fig. 8) the value of the stream function induced by the
image system $\overline{\psi}_1^{(i)}$ must be obtained. Along the shoulder characteristic
CD we have the relation

$$\tfrac{2}{3} \eta^{\frac{3}{2}} + (\theta - \theta_0) = 0 \qquad (III.5)$$

For the calculations it is desirable to obtain a relation between
f_m and ξ_m as well as a relation between ξ_m and θ/θ_0 valid
along the shoulder characteristic CD. By manipulation of the last
three equations we obtain

$$f_m = \tfrac{3}{2} \theta_0 \left\{ \frac{1 \mp \xi_m^{\frac{3}{2}}}{1 \pm \xi_m^{\frac{3}{2}}} \right\} \qquad (III.6)$$

and

$$\frac{\xi_m^{\frac{3}{2}}}{\xi_m^{\frac{3}{2}} \mp 1} = \frac{1 - \theta/\theta_0}{2|m| \mp 1} \qquad (III.7)$$

with the upper sign for positive m and lower sign for negative m and
m = 0. Then one can rewrite Eq. (III.2) as

$$\overline{\psi}_1^{(i)} = \sum_m \left(\tfrac{3\theta_0}{2} \right)^{-\frac{5}{3}} \left(2|m| \pm 1 \right)^{-\frac{4}{3}} \left\{ \frac{1 \pm \xi_m^{\frac{3}{2}}}{1 \mp \xi_m^{\frac{3}{2}}} \right\} G\left\{ \xi_m, \left(\tfrac{9}{4} + 3 \right)^2 \right\} \qquad (III.8)$$

For the practical computations one plots the expression

$$\left\{\frac{1\pm\xi_m^{\frac{3}{2}}}{1\mp\xi_m^{\frac{3}{2}}}\right\}^{-\frac{5}{6}} G\left\{\xi_m, \left(\frac{q}{4}+3\right)^2\right\} \quad \text{versus} \quad \frac{\xi_m^{\frac{3}{2}}}{\xi_m^{\frac{3}{2}}\mp 1}$$

From this curve one can obtain the expression occurring in Eq. (III.8). Because of Eq. (III.7) the abscissa for a given θ can be computed for different values of m very simply. The values of the stream function induced by the image system $\overline{\psi}_i^{(1)}$ is presented by the solid line in Fig. 10.

To fulfill the boundary conditions ψ = 0 along the shoulder characteristic CD a system of Chapligin solutions $\overline{\psi}_i^{(2)}$ is superimposed to the image system $\overline{\psi}_i^{(1)}$. In Section IV the Chapligin solutions were chosen in such a manner that they fulfill the boundary condition ψ = 0 along θ = 0 and $\theta = \theta_o$.

$$\psi_i^{(2)} = \sum_m a_m g(\eta, m) \sin\frac{m\pi\theta}{\theta_o} \qquad (III.9)$$

The coefficients a_m must be determined to satisfy along the shoulder characteristic CD the condition:

$$\overline{\psi}_i^{(1)} + \overline{\psi}_i^{(2)} = 0 \qquad (III.10)$$

In the fulfillment of this condition we deviate from the procedure used in Ref. 2. In that paper a rather ingeneous procedure was devised by which the determination of the coefficients a_m was reduced to a number of Fourier analyses. It appeared that a direct fulfillment of the boundary conditions along the Mach wave CD might be more exact and not involve a larger amount of numerical work. A finite number of coefficients a_m will be determined in such a manner that along CD the square of the

deviations of the left hand side of Eq. (III.10) is minimized. Rather than using the integral over the square of the deviations it is more practical to minimize the sum of the same quantity over a finite number of points (in this paper 47 points). The list of the resulting values obtained for a_m is presented in Table I. The circled points on Fig. 10 give the negative sum of the Chapligin solutions for comparison. The agreement is very satisfactory in the main part of the graph, particularly since the subsonic region seems to be quite insensitive to an error in the fulfillment of the boundary conditions in the supersonic region.

The solution is given by

$$\bar{\psi}_1 = \bar{\psi}_1^{(1)} + \bar{\psi}_1^{(2)} \tag{III.11}$$

It remains to evaluate the quantities of physical interest, i.e., the deviations of the pressure distribution over the wedge caused by the perturbation solution.

In preparation for determining this pressure distribution, it is necessary to calculate the value of $\bar{\psi}_1$ along the limiting characteristic OD. The limiting characteristic OD has the equation

$$\frac{2}{3} \eta^{\frac{3}{2}} - \theta = 0 \tag{III.12}$$

The quantities ξ_m and $\mathcal{P}_m$ are again introduced by Eq. (III.3) and Eq. (III.4). Then along the limiting characteristic one obtains

$$\mathcal{P}_m = \left\{ \frac{3}{2} \theta_0 |2m| \right\}^2 \left\{ \frac{1 \mp \xi_m^{-\frac{3}{2}}}{1 \mp \xi_m^{\frac{3}{2}}} \right\} \tag{III.13a}$$

and

$$\frac{\xi_m^{\frac{3}{2}}}{1 \pm \xi_m^{\frac{3}{2}}} = \frac{\theta/\theta_o}{2|m|} \qquad\qquad \text{(III.13b)}$$

The connection between upper and lower signs and the values of m are the same as previously. Consequently the mth term of the series may be written

$$\left\{ \tfrac{3}{2}\theta_0 |2m| \right\}^{-\frac{11}{3}} \left\{ \frac{1 \pm \xi_m^{\frac{3}{2}}}{1 \mp \xi_m^{\frac{3}{2}}} \right\}^{-\frac{5}{6}} G \left\{ \xi_m, \left(\tfrac{9}{4}+3\right)^2 \right\} \qquad \text{(III.14)}$$

The case that m = 0 must be considered separately and in obtaining $\overline{\psi}_1^{(1)}$ for m = 0 we utilize Eq. (18d) of Ref. 1 with the eigen value of our problem $(9/4 + 3)^2$. Along the limiting characteristic OD we have $\xi = 1$. Thus one obtains immediately the simplified expression

$$\overline{\psi}_{m=0}^{(1)} = \Gamma\left(\tfrac{1}{2}\right) \rho_{m=0}^{-\frac{11}{6}} \frac{\Gamma\left(-\tfrac{7}{2}\right) \sin\left(-\tfrac{3\pi}{2}\right)}{\Gamma\left(-\tfrac{5}{6}\right)\Gamma\left(-\tfrac{7}{6}\right)} \left(1-\xi^3\right)^{-\frac{11}{6}} \qquad \text{(III.15)}$$

as $\quad \xi \to 1$

Since

$$\rho = \left(\tfrac{3}{2}\theta\right)^{-\frac{11}{3}} \left(1-\xi^3\right)^{-\frac{11}{6}} \qquad\qquad \text{(III.16)}$$

One obtains after manipulating the Γ functions for m = 0

$$\overline{\psi}_{m=0}^{(1)} = \left(\tfrac{3}{2}\theta\right)^{-\frac{11}{3}} \left(-\tfrac{1}{81}\right) \qquad\qquad \text{(III.17)}$$

along line $\xi = 1$. With these results $\overline{\psi}_1^{(1)}$ along the limiting characteristic will be computed in a manner quite similar to the computations along the shoulder characteristic. Furthermore the Chapligin solutions must be superimposed. Results of this computation are presented in Fig. 11.

To obtain the pressures along the front part of the wedge it is necessary to determine the x coordinates. This can be accomplished in terms of the stream function by means of integration, however, it is more convenient to utilize the transformed potential. This can be done directly because of the relation between the stream function and the transformed potential in Eq. (3.8). If the transformed potential is known one can obtain the x coordinate by differention and Eq. (3.11). In the present approximation φ fulfills the same differential equation as ψ and thus it is to be expected that the expression for φ which corresponds to a particular solution ψ has the same form with changed values of the eigen values λ_h. Specifically the expression for

$$\psi = \rho^{-\frac{4}{6}} \, G^{(a)} \left\{ \xi, \, \left(\frac{9}{4}+3\right)^2 \right\} \tag{III.18}$$

Setting ρ^{λ} equal to one then the corresponding expression for φ is given by:

$$\varphi = -\frac{3}{40} \, \rho^{-\frac{4}{3}} \, G^{(s)} \left\{ \xi, \, \left(\frac{3}{4}+3\right)^2 \right\} \tag{III.19}$$

This is the expression which will be used for the further computations.

The expression $\overline{\varphi}_{,}^{(2)}$ which corresponds to the Chapligin solution for the stream function Eq. (III.9) is found to be

$$\overline{\varphi}_{,}^{(2)} = \sum_m a_m \, \frac{\theta_o}{m\pi} \, g(\eta, m) \cos \frac{m\pi\theta}{\theta_o} \tag{III.20}$$

In the calculation of the x coordinate along the subsonic portion of the wedge it is necessary to determine $\overline{\varphi}_{,\eta}$ along $\theta = \theta_o$. From Eq. (III.3) and Eq. (III.4) one finds for the mth singularity

$$\rho_m = \eta^3 \left\{ \frac{1 - \xi_m^3}{\xi_m^3} \right\} \tag{III.21a}$$

$$\xi_m = \frac{\eta}{\left[|2m \pm 1| \theta_0 \right]^{\frac{3}{2}}} \tag{III.21b}$$

With some manipulation with Eq. (III.19) one finds for the mth term of the image system along $\theta = \theta_0$.

$$-\frac{3}{40} \left(\frac{3\theta_0}{2} \right)^{-\frac{10}{3}} \left[|2m \pm 1| \right]^{-\frac{10}{3}} \left\{ \frac{4\xi_m^2}{(1 - \xi_m^3)^{\frac{2}{3}}} G(\xi_m, \lambda) + \frac{G'(\xi_m, \lambda)}{(1 - \xi_m^3)^{\frac{4}{6}}} \right\} \tag{III.22}$$

When $\xi < -1$, an independent variable w has been introduced instead of

ξ , i.e., $w = (-\xi)^{-\frac{3}{2}}$ then the mth term of $\overline{\varphi}_{,\eta}^{(1)}$ is expressed as:

$$-\frac{3}{40} \left(\frac{3\theta_0}{2} \right)^{-\frac{10}{3}} (|2m \pm 1|)^{-\frac{10}{3}} \left\{ \frac{w^{\frac{10}{3}}}{(1 + w^2)^{\frac{2}{3}}} \right\} \left[4 g(w, 0) + \frac{3}{2} (1 + w^2) \frac{dg(w, 0)}{dw} \right] \tag{III.23}$$

The values of $\overline{\varphi}_{,\eta}^{(1)}$ produced along the line $\theta = \theta_0$ in the

subsonic region by the image system as calculated by the summation are

presented in Fig. 12. To this summation the contribution of the Chapligin

solutions must be superimposed. The mth term of the Chapligin solution

has the form

$$\frac{a_m \theta_0}{m \pi} \frac{dg(\eta, m)}{d\eta} \cos \frac{m \pi \theta}{\theta_0} \tag{III.24}$$

where $\frac{dg(\eta, m)}{d\eta}$ is expressed in Eq. (4.6). The superimposition of the

two expressions $\overline{\varphi}_{,\eta}^{(1)}$, $\overline{\varphi}_{,\eta}^{(2)}$ along the line $\theta = \theta_0$ is presented in

Fig. 12. This curve gives $\overline{\varphi}_{,\eta}$ which belongs to the expression ψ_1

defined in Section VII.

To complete the computations of the subsonic part of the wedge

we need the value of $\overline{\varphi}_{0,\eta}$ produced by the basic solution ψ_0 . This

is shown in Fig. 13 for a singularity which is expressed by

$$\psi = \rho^{-\frac{5}{6}} \, G \left\{ \xi_m, \, \left(\tfrac{q}{4}\right)^2 \right\} \tag{III.25}$$

This curve is the same as used in the calculations of Ref. 2 except for a factor which comes in because of the different definitions of the singularity. These results were checked by the method developed in this paper and were found to be quite accurate.

According to the considerations discussed in Section VII such a portion k of $\overline{\varphi}_{o_\eta}$ for the basic potential was superimposed to the additional potential so that the sum of the value

$$k \, \overline{\varphi}_{o_\eta} + \overline{\varphi}_{1_\eta} = 0 \tag{III.26}$$

at the shoulder of the wedge $\eta = 0$. The curve thus obtained for the superimposed potential is presented in Fig. 12.

The next step in the computations will be the construction of the superimposed potential downstream of the limiting characteristic OD of Fig. 8. This will be done by the method of characteristics in a semigraphical form. This construction must naturally be carried out in the same region of the hodograph in which the potential of the basic flow had been found. Therefore, the construction of the basic flow will be discussed first. Only that part of the construction which affects the pressure on the surface of the wedge is shown.

Figure 14 represents the basic flow in the physical plane. (This is simplified version of Fig. 14 of Ref. 2.) The computation of the flow over the nose of the wedge includes the computation of the values of φ_η and φ_θ along the limiting characteristic ND. Therefore, in the corresponding η, θ graph the values of φ_θ and φ_η can be

considered as known. For simplicity we shall use in these discussions a graph in which $\eta^{\frac{3}{2}}$ is plotted versus θ Fig. 15. In this plot the characteristics appear as straight lines. At point D the velocity vector has a slope + $\theta_0/_2$ while at the rear part of the wedge it has the slope of - θ_0 . Therefore, an expansion will take place. This expansion over the shoulder of the wedge imposes the boundary condition that ψ = 0 along the characteristic DK. In Fig. 14 points D and K coincide and from this condition one finds immediately that φ_η = constant along this line. With these boundary conditions φ_θ and φ_η are determined in the characteristic quadrangle NDKL (see Fig. 14 and Fig. 15). In the physical plane this characteristic quadrangle corresponds to the region of the Meyer expansion denoted by the same letters. The characteristics of the same family as the limiting characteristic PQ are the Mach waves of the Meyer expansion, the characteristics of the same family as DK are the Mach waves which come from the sonic line. Since point O lies at infinity in the physical plane the Mach wave OR will also lie at infinity. Because of the relations of Eq. (3.11) and Eq. (3.12), Fig. 14 can be interpreted as a representation of the φ_θ , φ_η plane as well as of the physical plane. The characteristic conditions in the hodograph plane yield

$$\frac{d\varphi_\eta}{d\varphi_\theta} = \pm \sqrt{\eta} \qquad\qquad (III.28)$$

where the signs are used consistently with the equation for the direction of the Mach waves in the η, θ plane

$$\frac{d\eta}{d\theta} = \pm \sqrt{\eta} \qquad\qquad (III.29)$$

Equation (III.28) gives in a φ_θ , φ_η plane the directions of the

characteristics between two predetermined points of the η, θ plane. Thus Fig. 14 can be interpreted as a construction of φ_θ and φ_η by a graphical method.

Along the rear of the wedge, i.e., for $\psi = \varphi_\theta = 0$ we have in the physical plane $\theta = -\theta_o$. Translated into the corresponding condition in the η, θ plane is that along MK we have $\varphi_\theta = 0$. The construction in the physical plane shows how this condition will be fulfilled. The points of the region downstream of LK will be mapped into a second sheet of the η, θ plane which is connected to the first sheet along LK. The boundary condition along MK mentioned above will be imposed in the second sheet.

For the determination of the superimposed solution we need the values of $\overline{\varphi}_{,\eta}$ and $\overline{\varphi}_{,\theta}$ in the same regions, i.e., first in the region ADKL and then in the second sheet KLM.

The values of $\overline{\varphi}_{,\theta}$ for the additional potential are known along the limiting characteristic OD (Fig. 11). The values of $\overline{\varphi}_{,\eta}$ can be constructed in a $\varphi_\eta, \varphi_\theta$ graph using Eq. (III.28). In the total expression for the potential the line DK must correspond to the flow over the shoulder of the double wedge, i.e., in the total potential $\varphi_\theta = 0$ along DK. Since $\varphi_\theta = 0$ in the basic flow, it follows that in the additional flow one also has $\varphi_\theta = 0$ along DK. With this boundary condition the values of $\overline{\varphi}_{,\theta}$ and $\overline{\varphi}_{,\eta}$ can be constructed in the region NDKL. This is done in a $\varphi_\eta, \varphi_\theta$ plane (Figs. 16a and 16b). This construction must be carried over into the second sheet LKM. Since MK will correspond to the zero streamline also in the total flow one obtains the condition $\varphi_\theta = 0$ along MK in the superimposed flow, i.e., all the boundary conditions for the superimposed flow are of the same

nature as those of the basic flow. With these remarks the construction in the region LKM in Figs. 15 and 16 is understood. From the construction in Figs. 16a and 16b the values of $\overline{\varphi}_{1_\eta}$ along the rear of the wedge is obtained. Then $\overline{\overline{\varphi}}_{1_\eta}$ is obtained by the same linear combination between $\overline{\varphi}_{1_\eta}$ and $\overline{\varphi}_{0_\eta}$ as in the subsonic region. $\overline{\varphi}_{0_\eta}$ is shown in Figs. 13 and 18. The values of $\overline{\overline{\varphi}}_{1_\eta}$ are presented in Fig. 17.

TABLE I

LIST OF COEFFICIENTS OF SUPERPOSITION OF CHAPLIGIN SOLUTIONS $\overline{\psi}_1^{(2)}$

IN THE FORM $\sum a_m \, g(\eta, m) \, \sin \frac{m \pi \theta}{\theta_o}$

m	a_m
1	+.1422
2	+.02042
3	+.03945
4	+.60476
5	+.0184
6	-.000052
7	+.01422
8	-.00200
9	+.0111
10	-.0001

LIST OF FIGURES

Fig. 1   PHYSICAL PLANE SOLID WALL TUNNEL
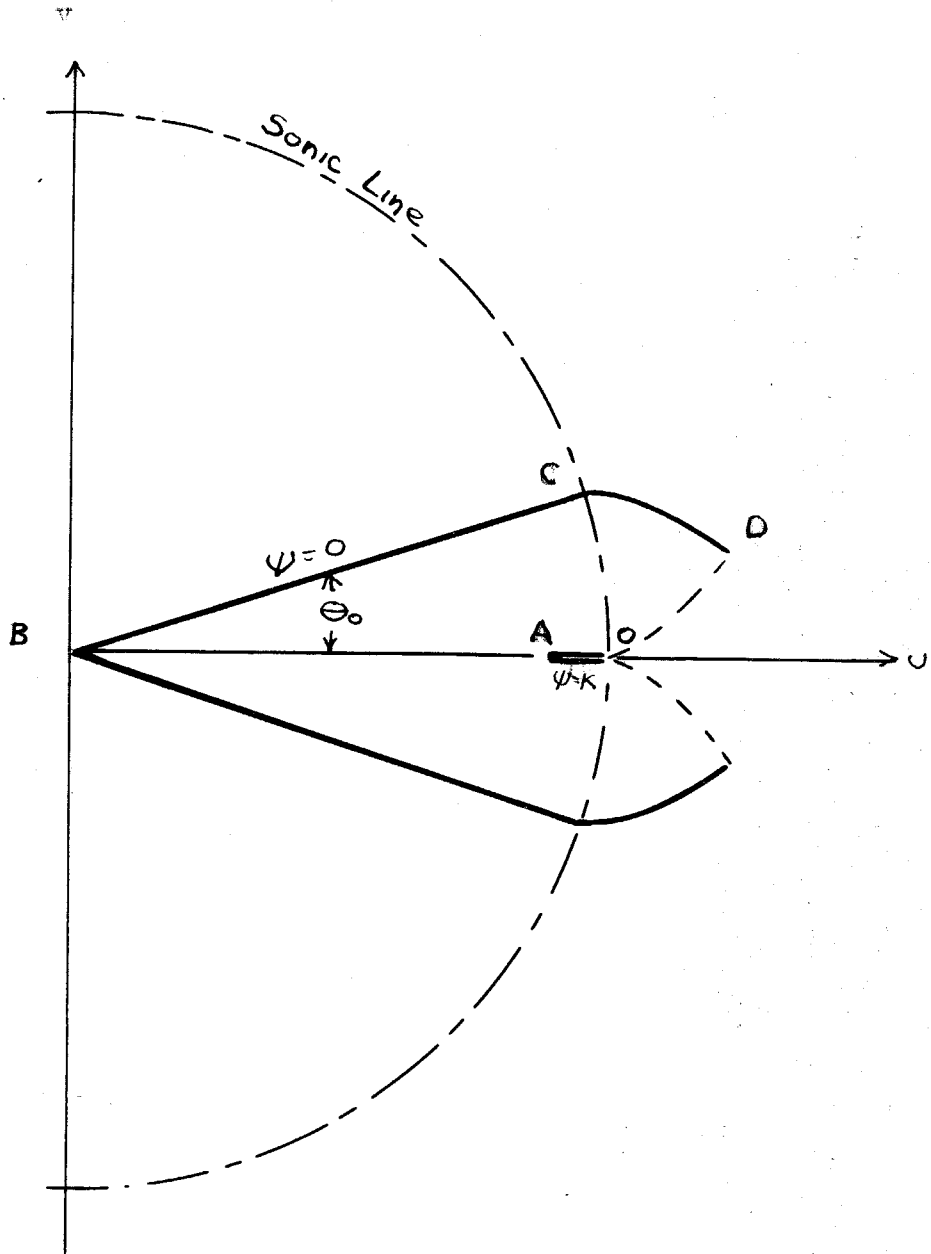
Fig. 2 HODOGRAPH PLANE SOLID WALL TUNNEL
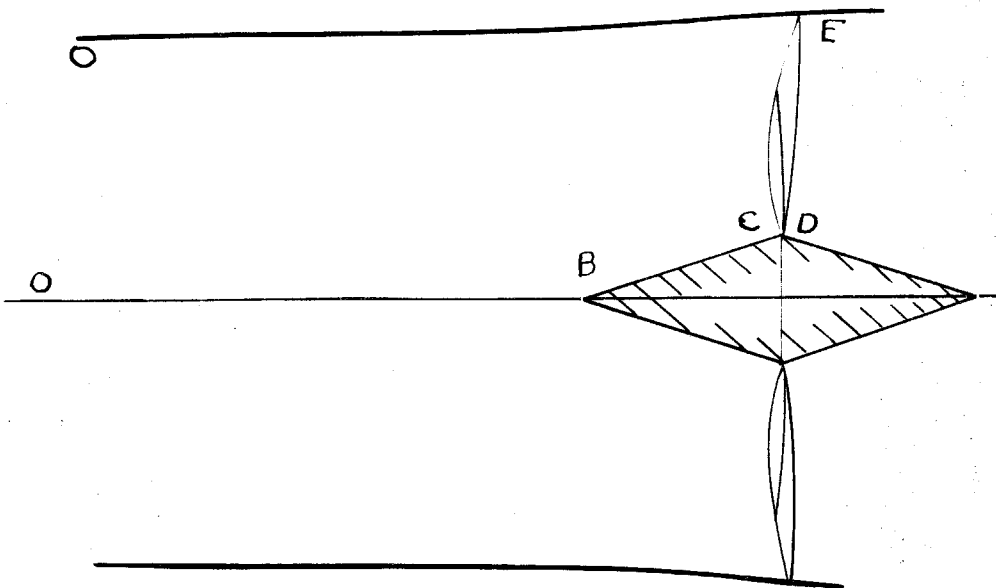
Fig.3   PHYSICAL PLANE ECHO FREE - JET
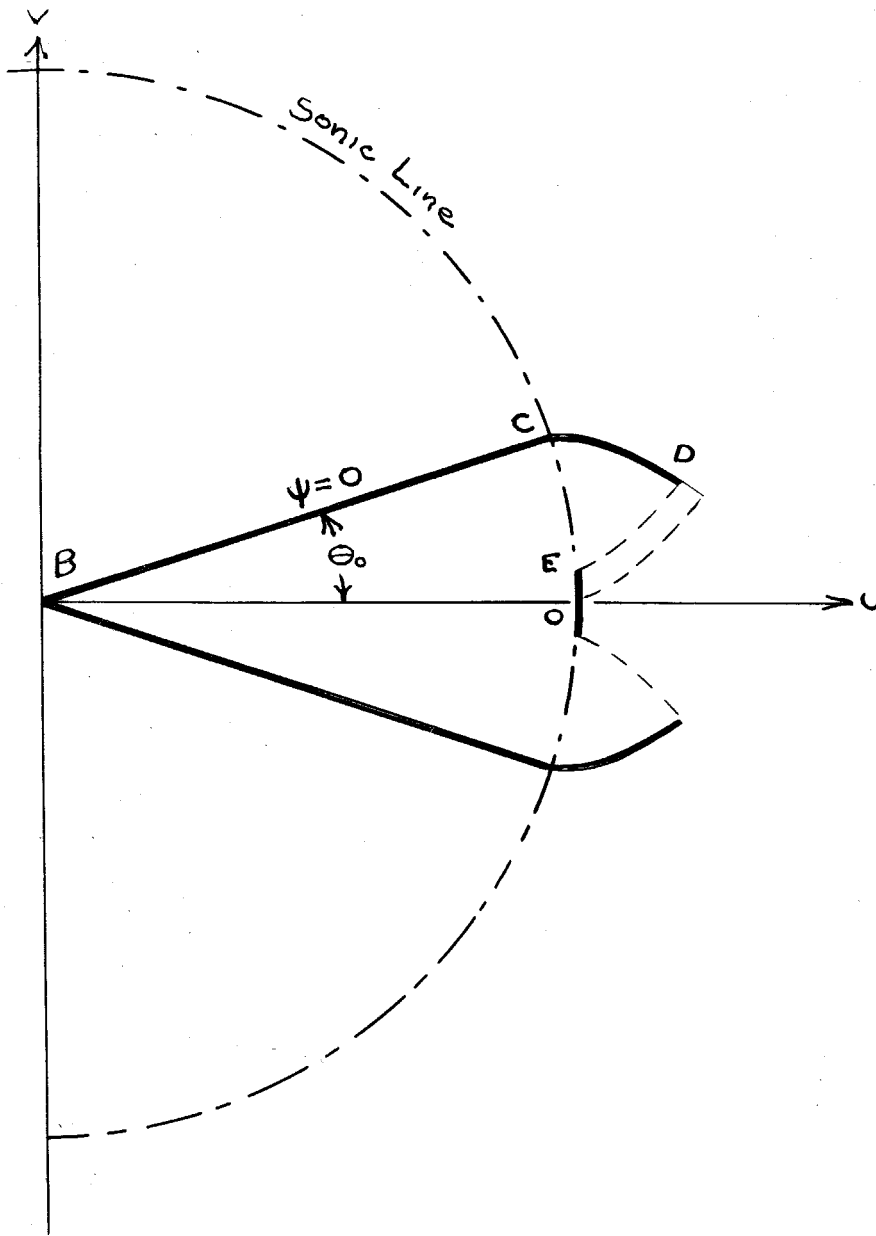
FIG. 4   HODOGRAPH PLANE SONIC FREE-JET

FIG. 5 TRANSONIC HODOGRAPH PLANE SOLID WALL TUNNEL

Fig. 6   TRANSONIC HODOGRAPH PLANE SONIC FREE-JET
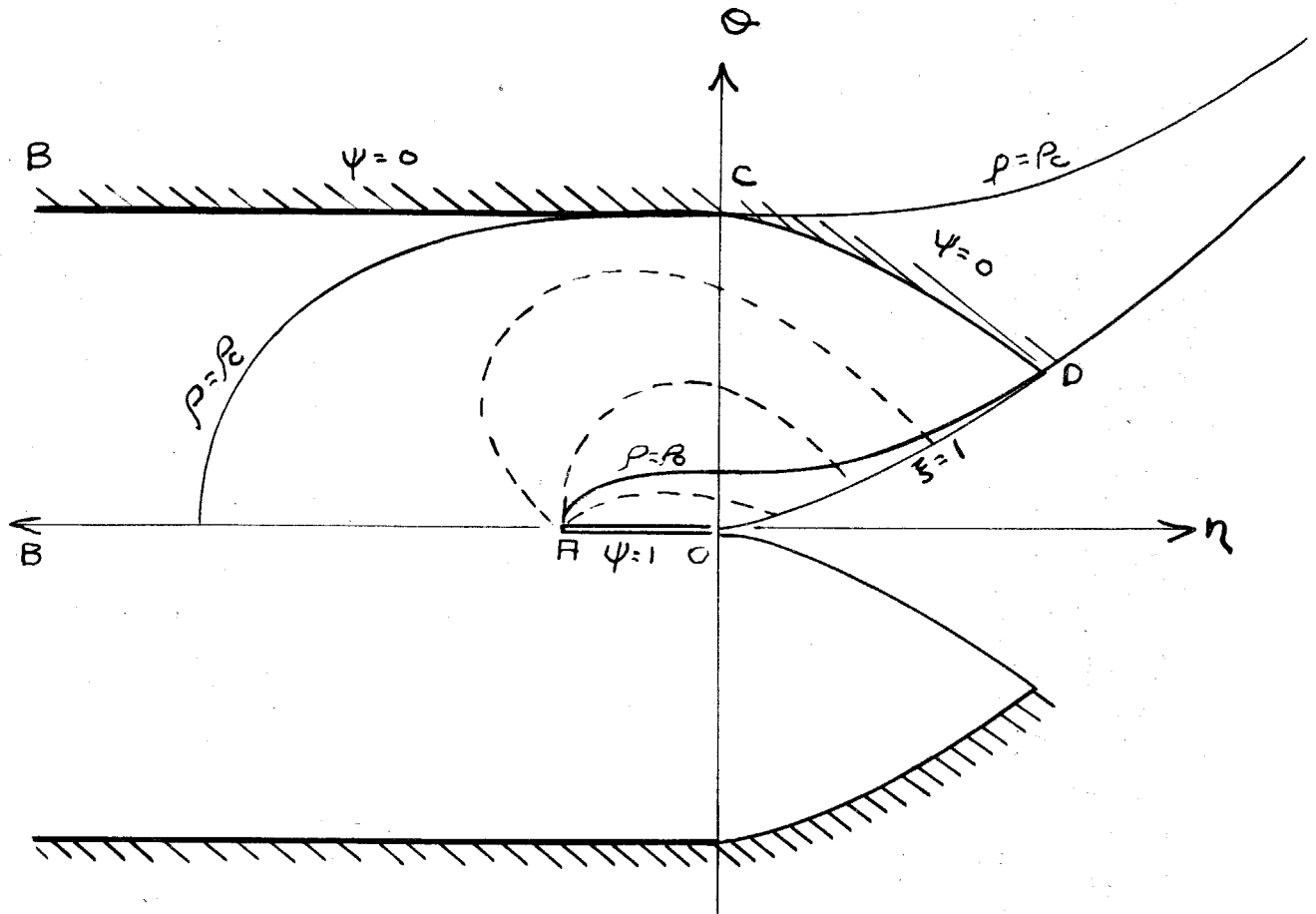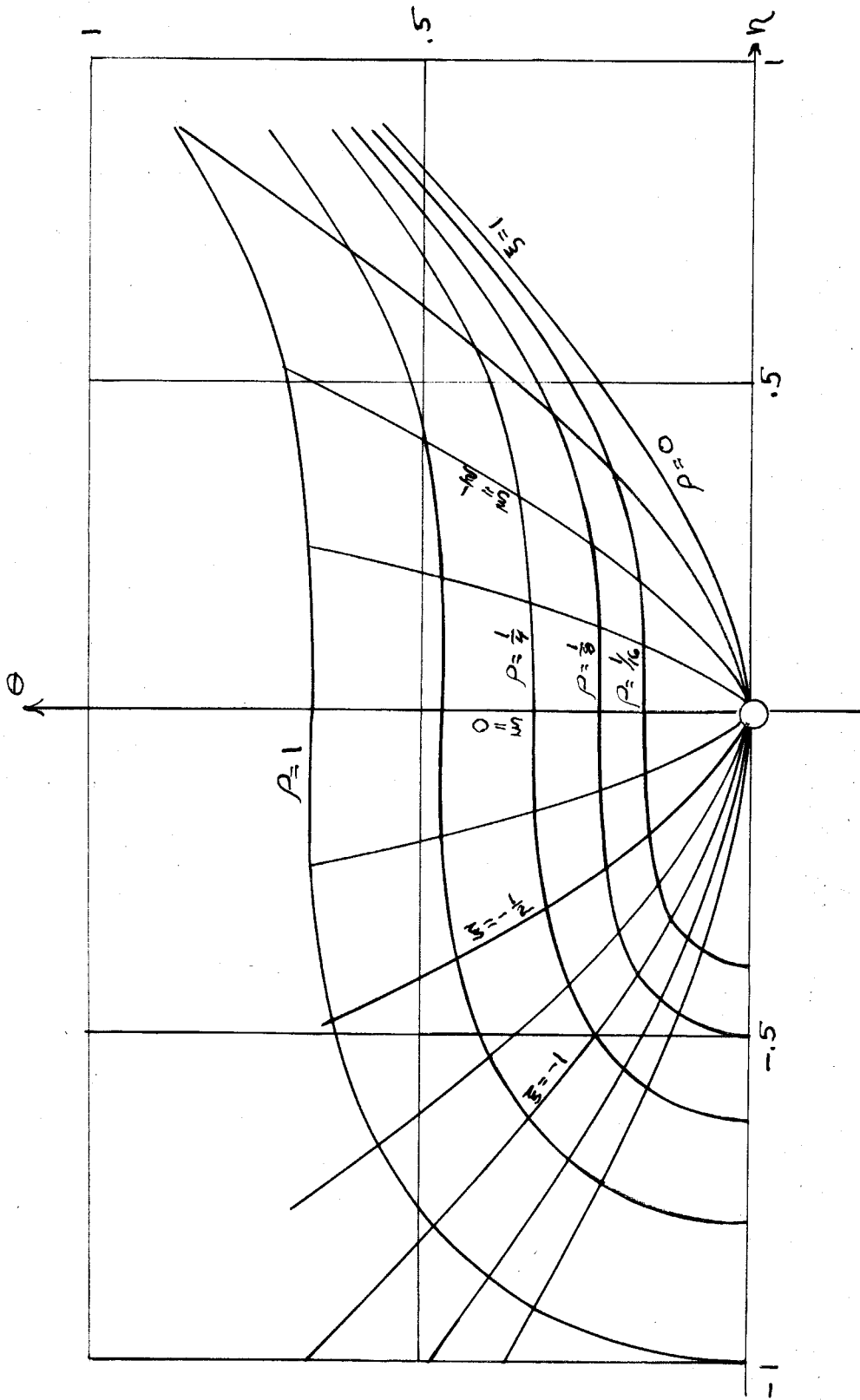
Fig. 7 ρ and ξ COORDINATE SYSTEM
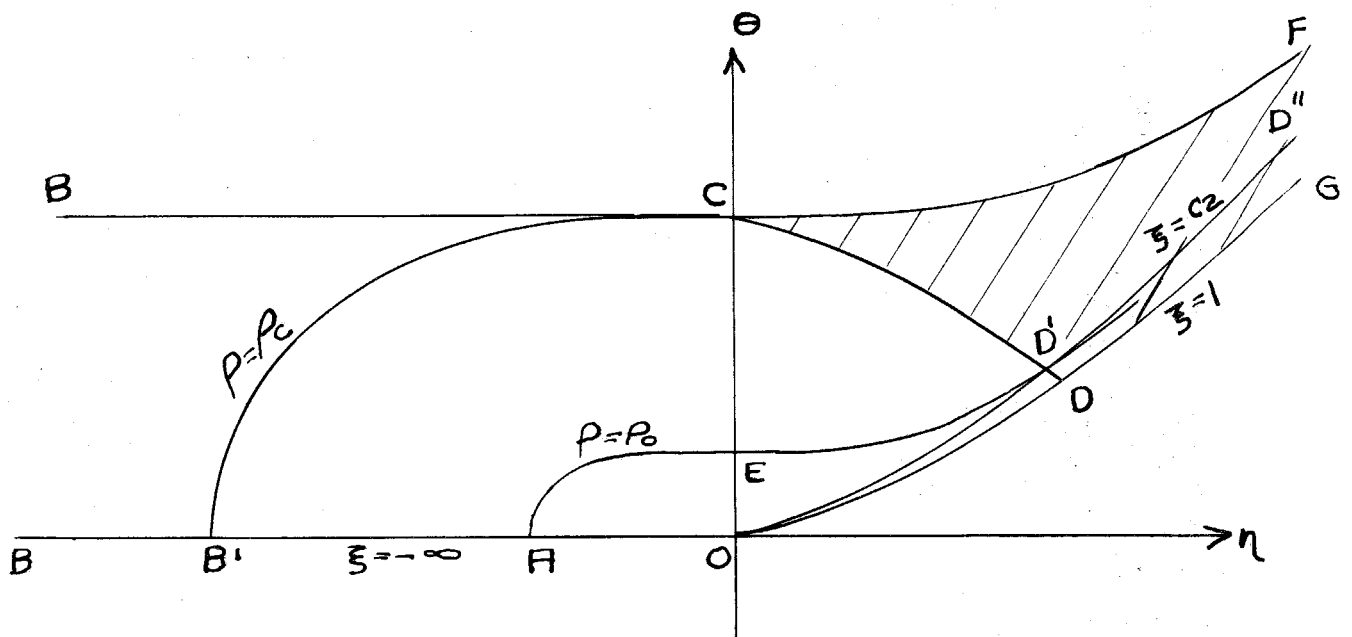
Fig. 8   GENERAL TRANSONIC BOUNDRY MAP IN η, θ PLANE
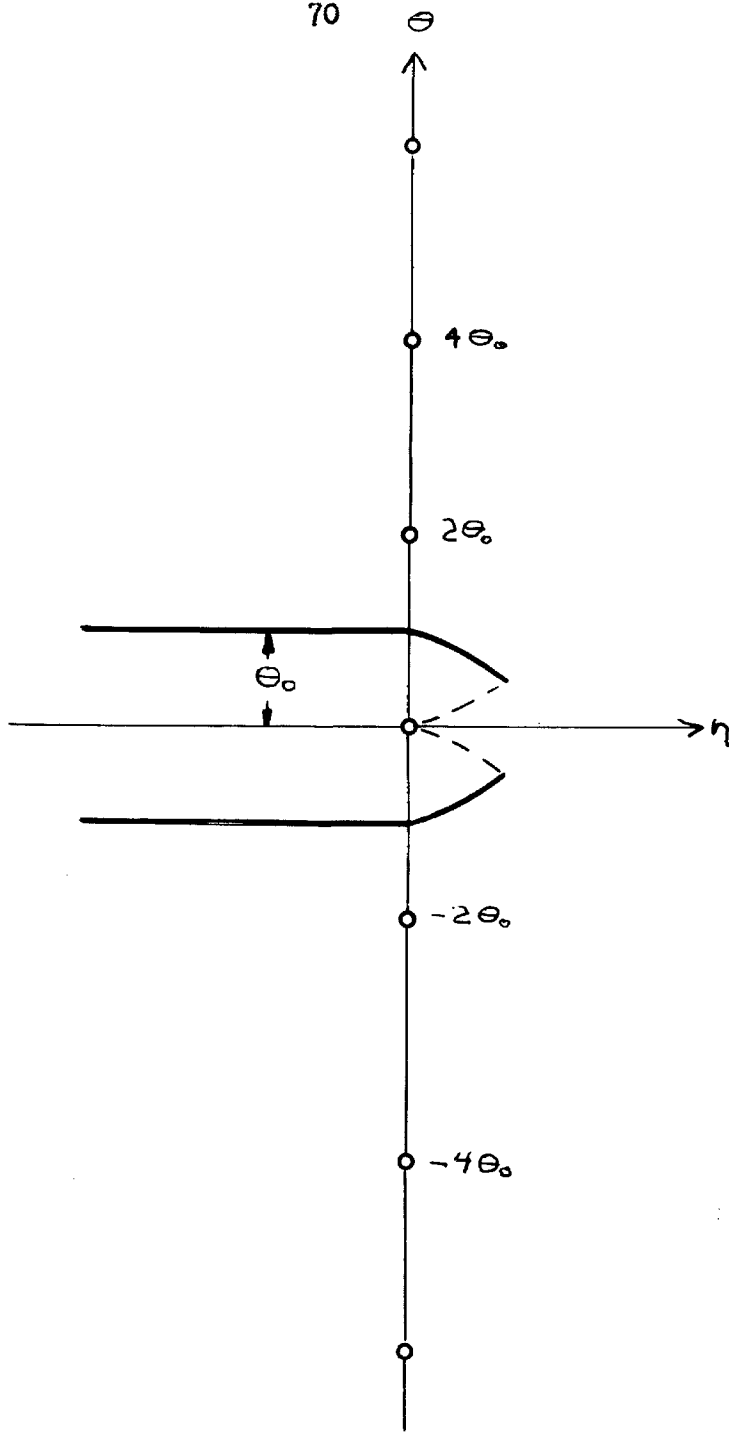
Fig. 9 IMAGE SYSTEM OF SINGULARITIES
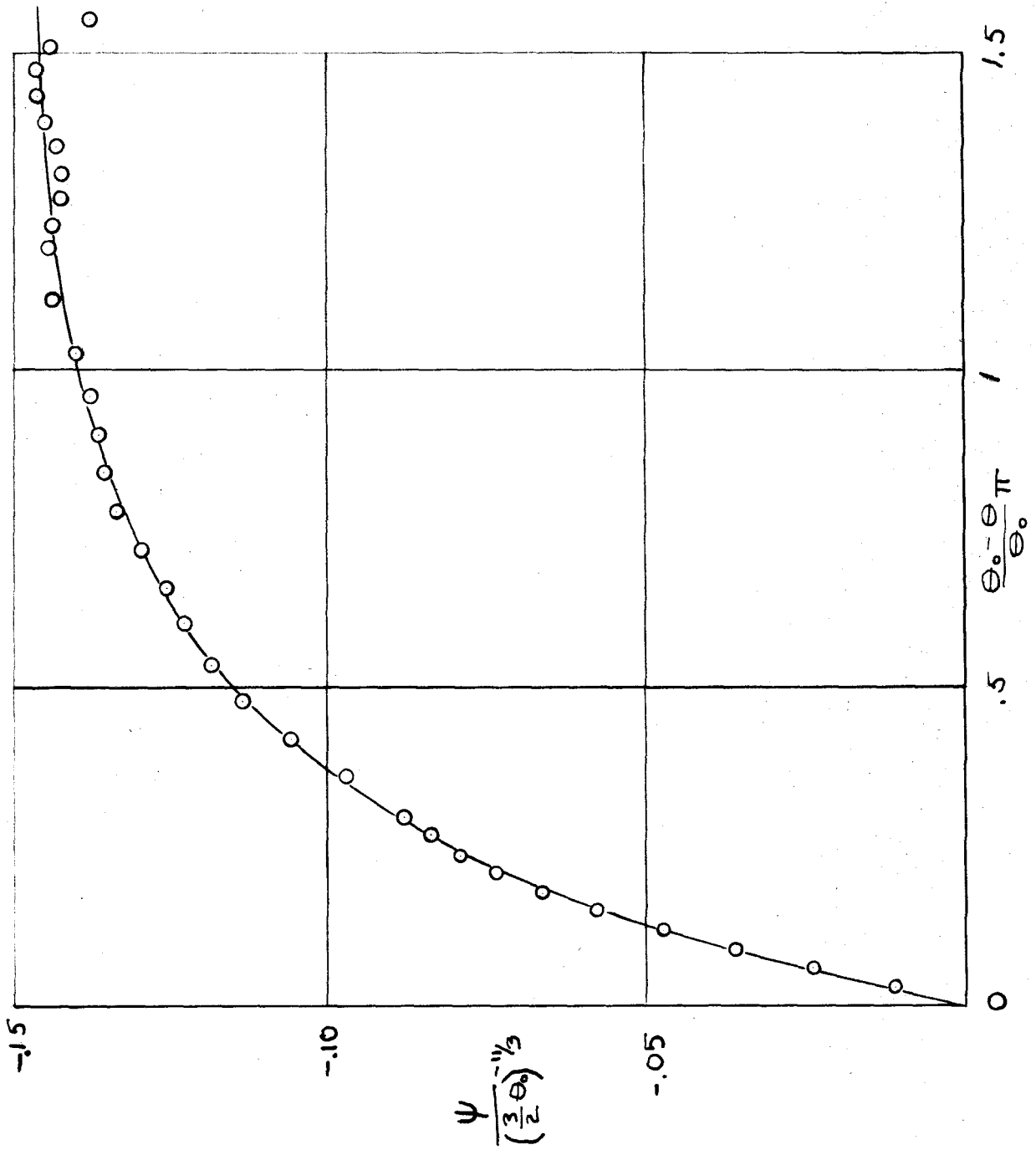
Fig. 10 DISTRIBUTION OF BOUNDARY CONDITIONS ALONG SHOULDER CHARACTERISTIC
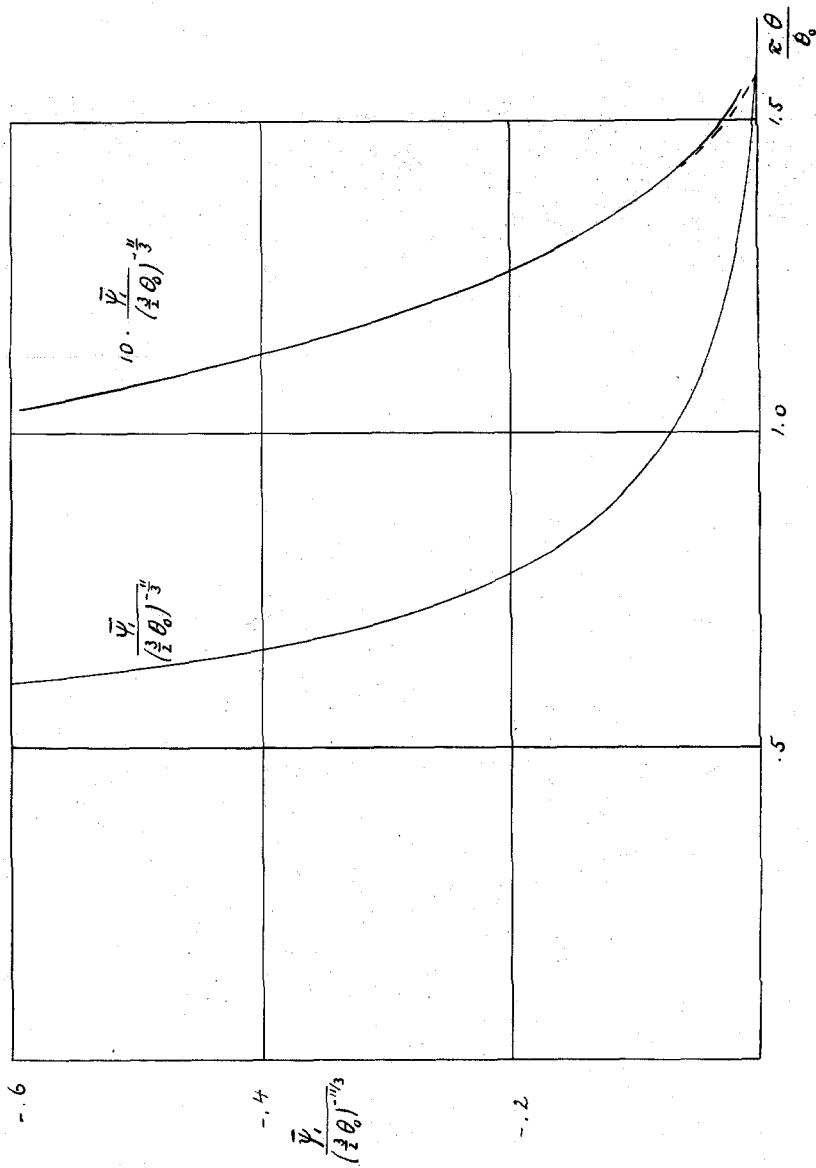
Fig. 11 STREAM FUNCTION $\overline{\psi}_1$ ALONG THE LIMITING CHARACTERISTIC
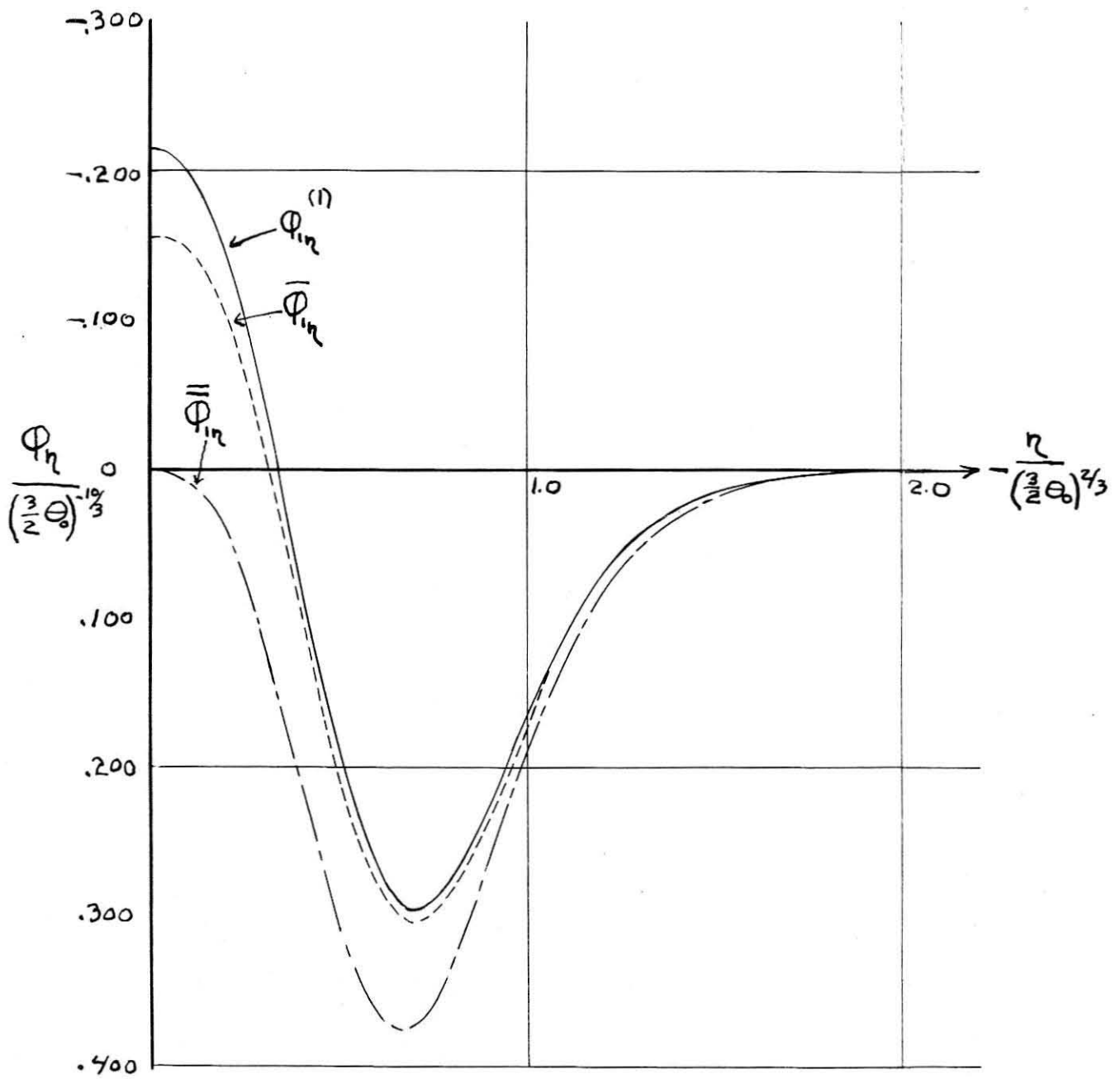
Fig. 12 φ_η ALONG SUBSONIC PART OF THE WEDGE
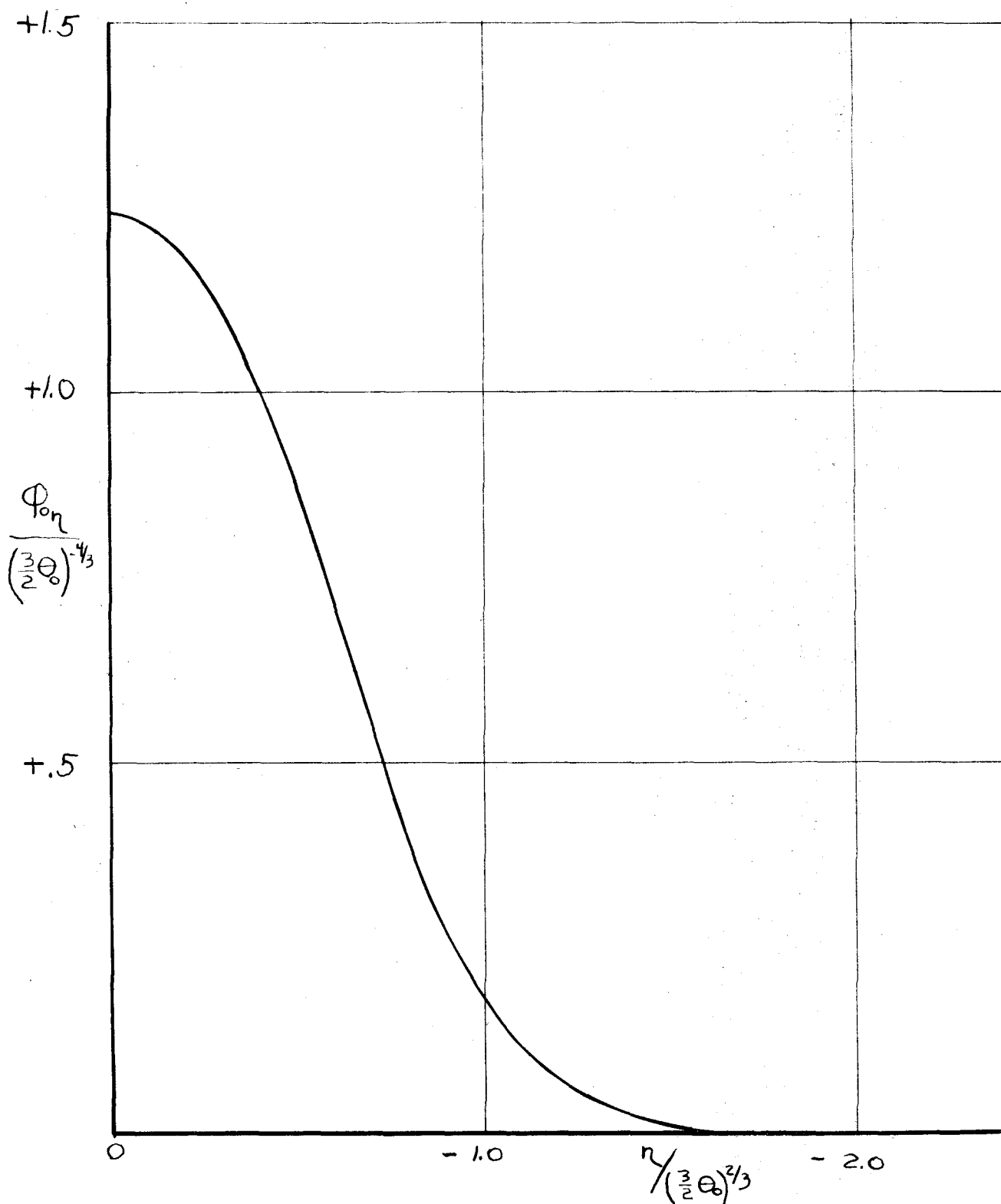
FIG. 13 $\varphi_{o\eta}$ ____ __ ___ ___ __ ___
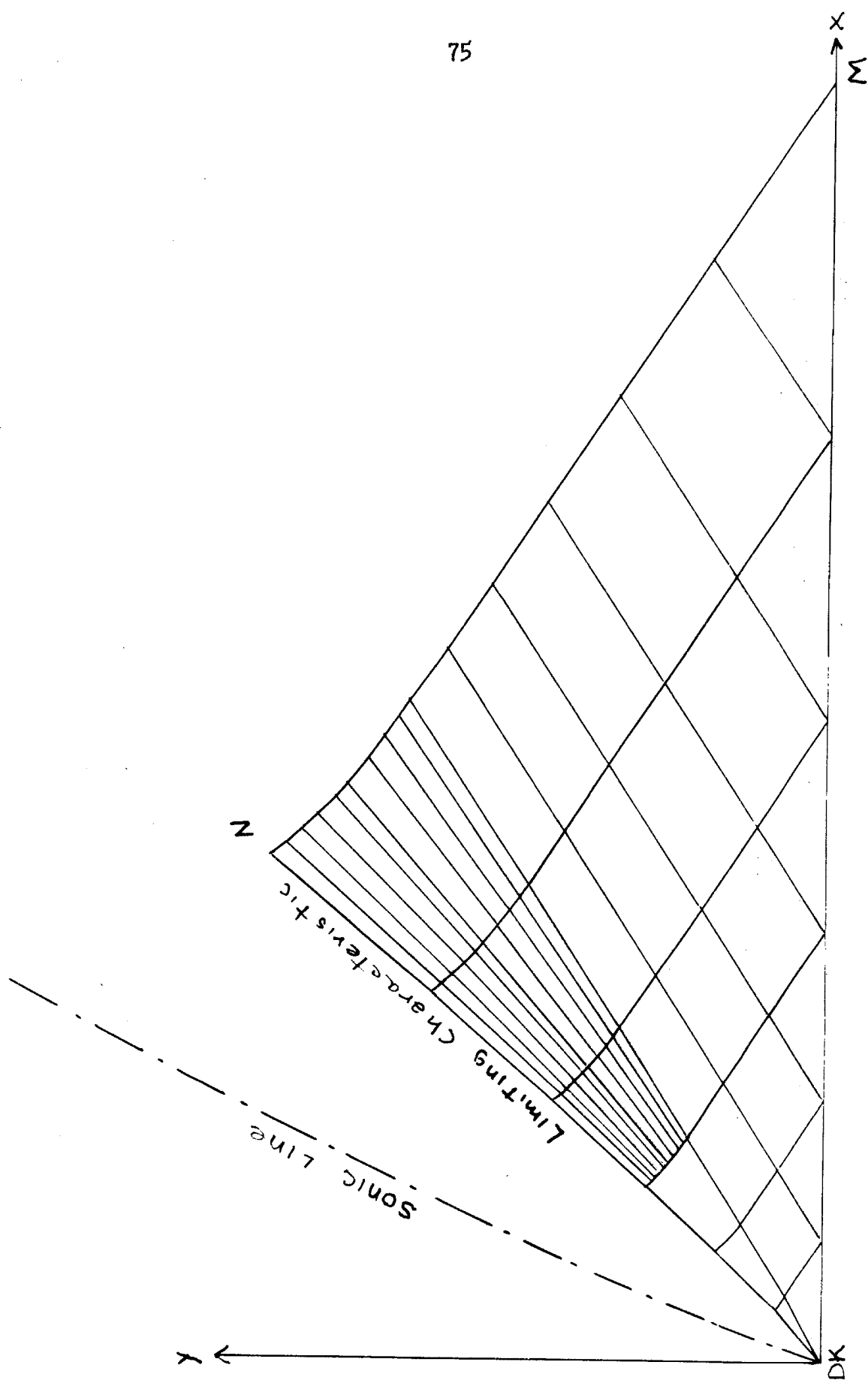
Fig. 14 CONSTRUCTION OF AREA OF WEDGE FLOW FOR EACH NUMBER ONE CASE
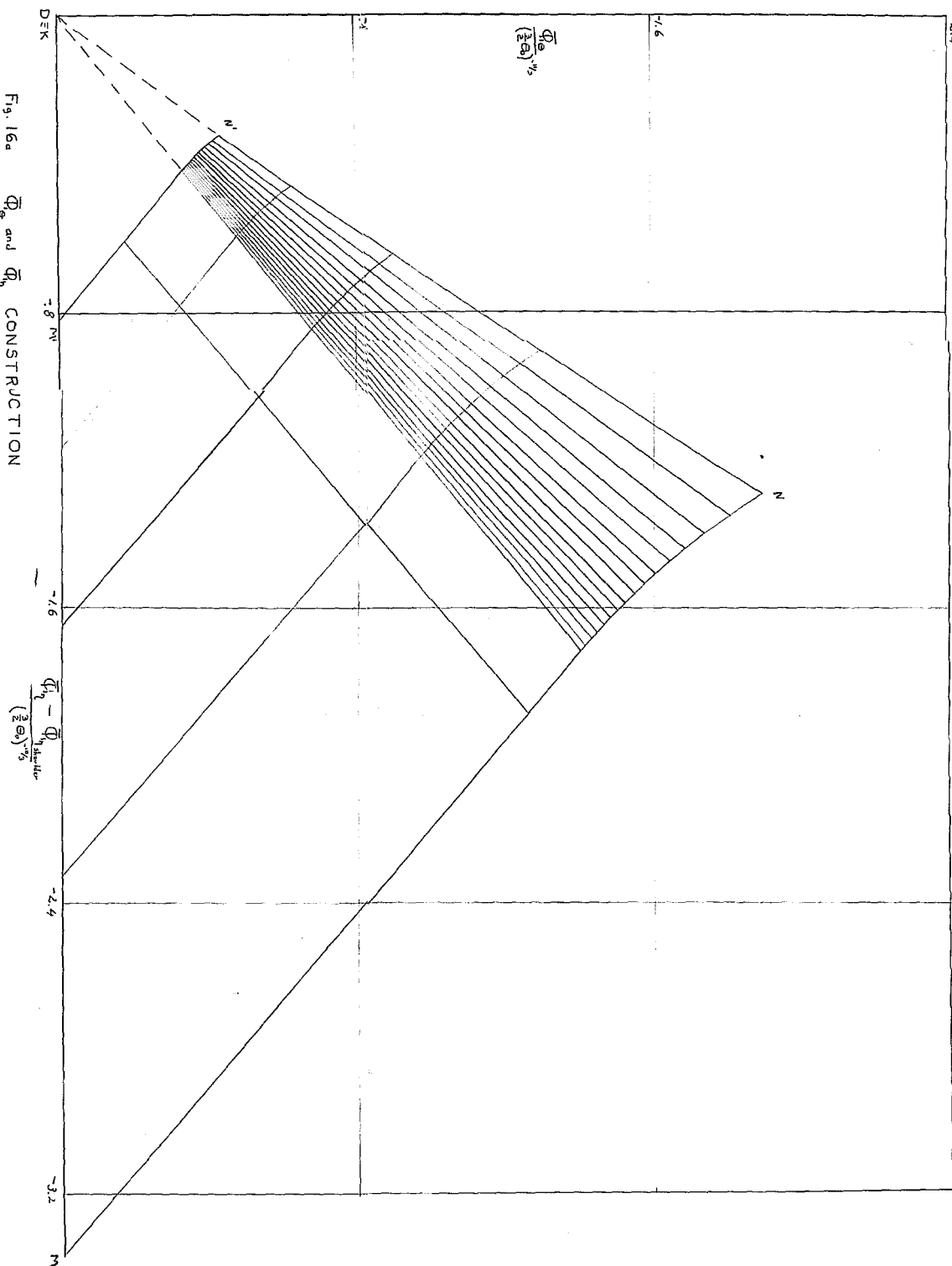
Fig. 15 CHANGE IN POSITION OF HYSTERESIS LOOP

Fig. 16a Φ_e and Φ_h CONSTRUCTION

Fig 16b $\overline{\Phi}_{ie}$ and $\overline{\Phi}_{in}$ CONSTRUCTION

$$\frac{\overline{\Phi}_{in} - \overline{\Phi}_{in \, shoulder}}{\left(\frac{3}{2}\theta_o\right)^{-10/3}}$$

$\left|\overline{\Phi}_e\left(\frac{3}{2}\theta_o\right)^{7/3}\right|$

$$\frac{\Phi_n}{\left(\frac{3}{2}\theta_0\right)^{-\frac{1}{3}}}$$

$$\eta/(\tfrac{3}{2}\theta_0)^{\frac{1}{3}}$$
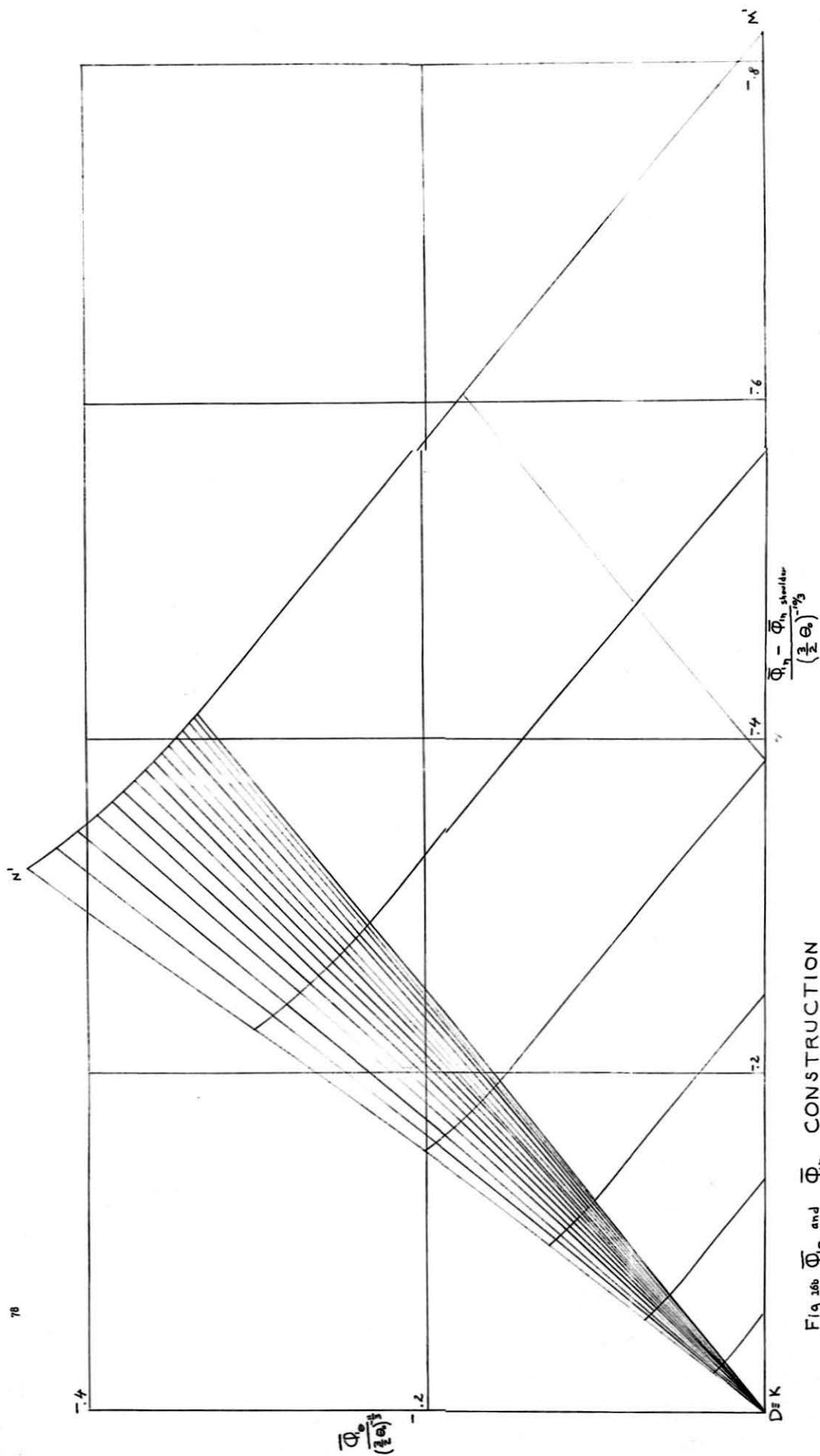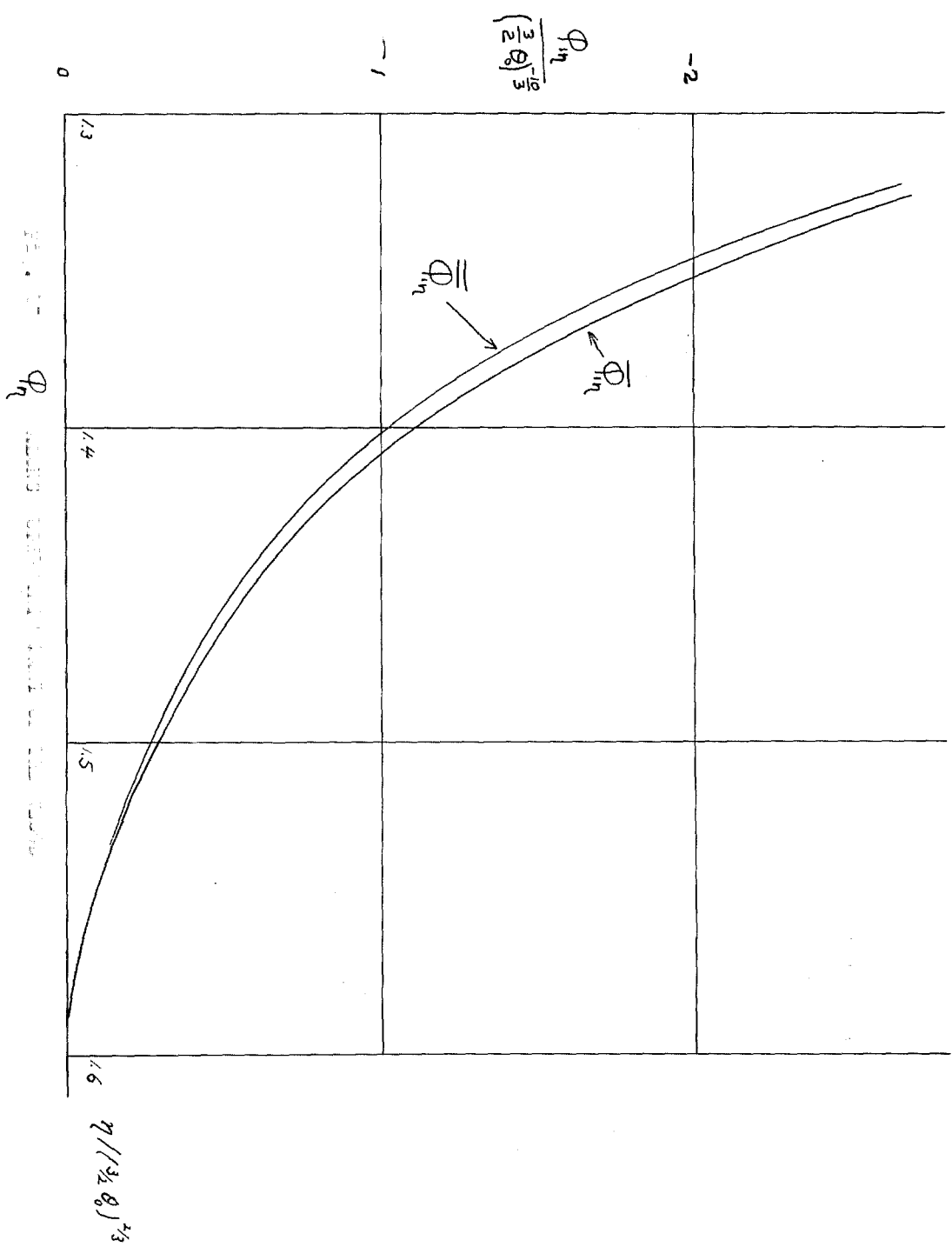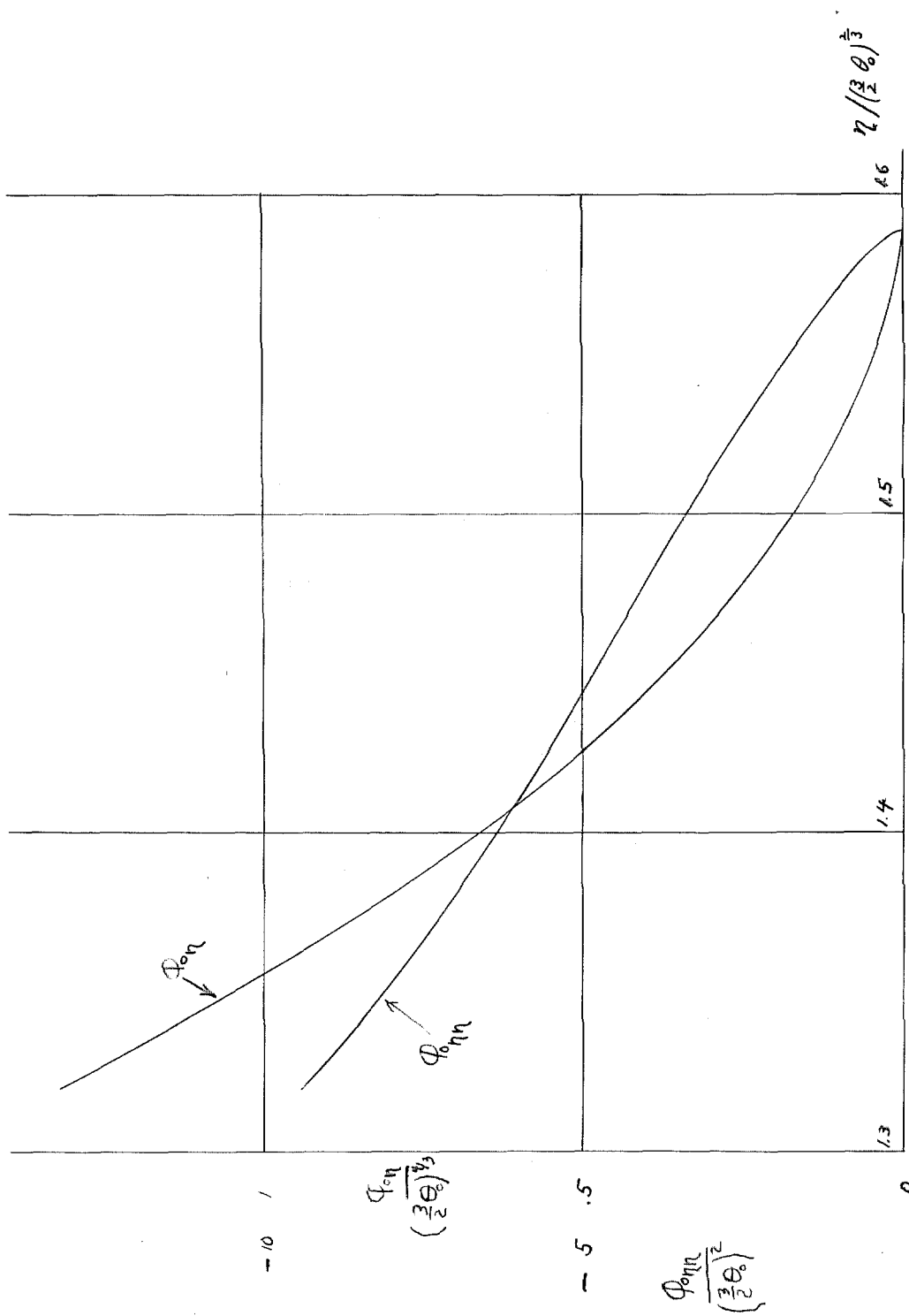
Fig. 18   COMPUTATION OF BASIC SINGULARITY
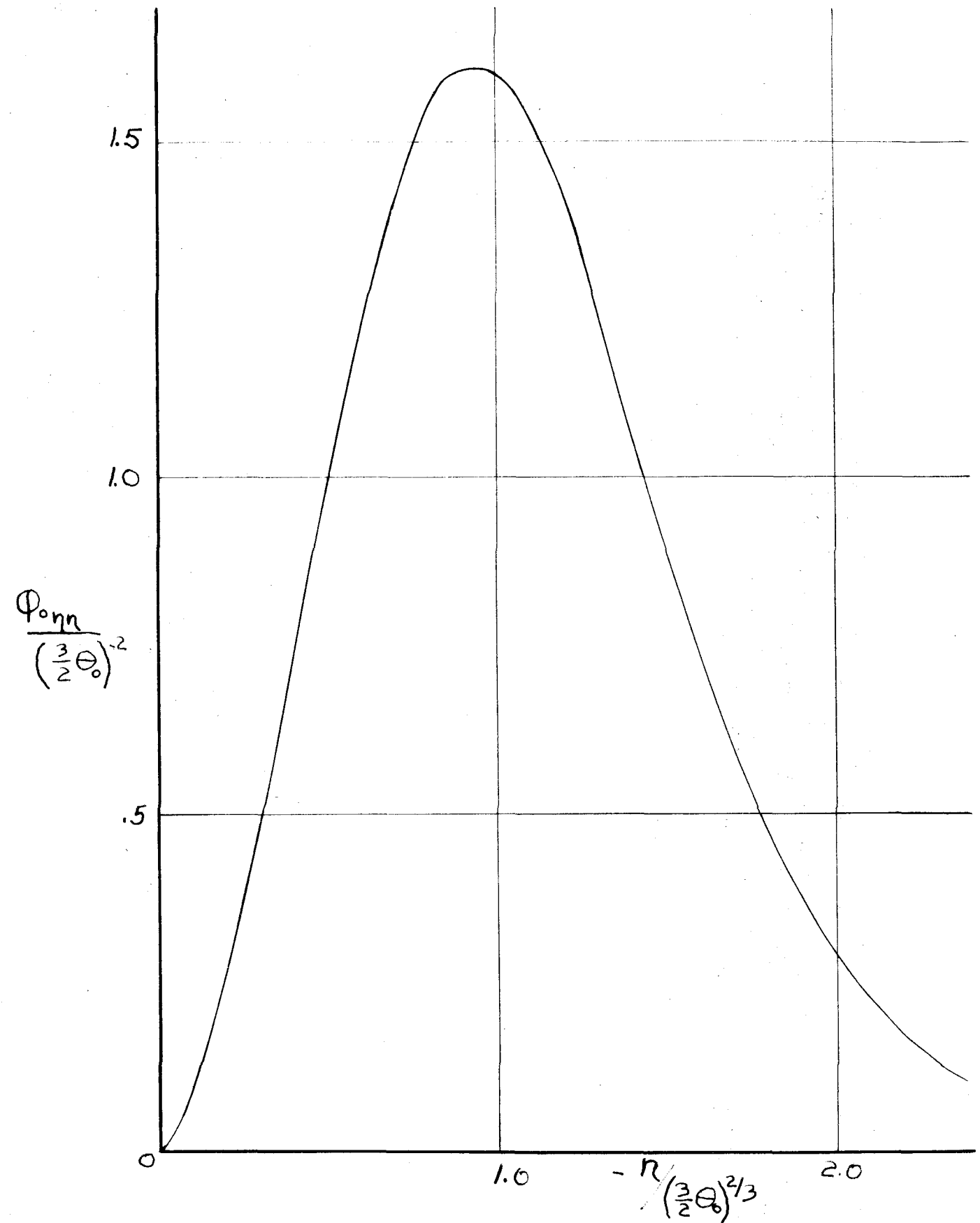
Fig. 16 $\Phi_{0\eta\eta}$ Along Subsonic Part Of The Seize

$$\Delta\eta = -\frac{\beta_l}{\beta_0}\left(\frac{3}{2}\theta_0\right)^{-4/3} F\left(\frac{X}{L}\right)$$
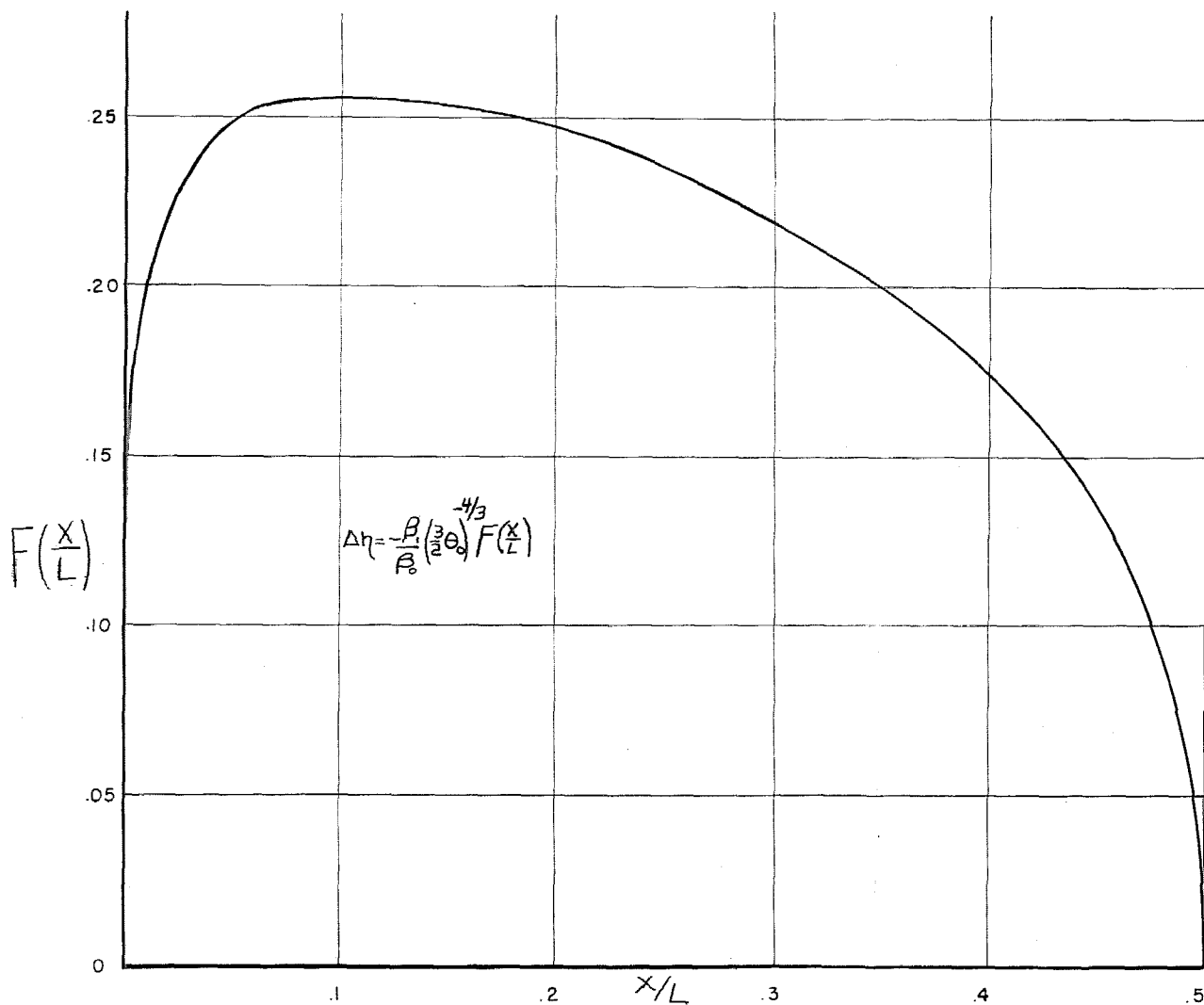
Fig. 40 $\Delta\eta$ ALONG FORWARD PART OF THE WEDGE

$$\Delta\eta = -\frac{\beta}{\beta_0}\left(\frac{3}{2}\theta_0\right)^{-4/3} F\left(\frac{x}{L}\right)$$
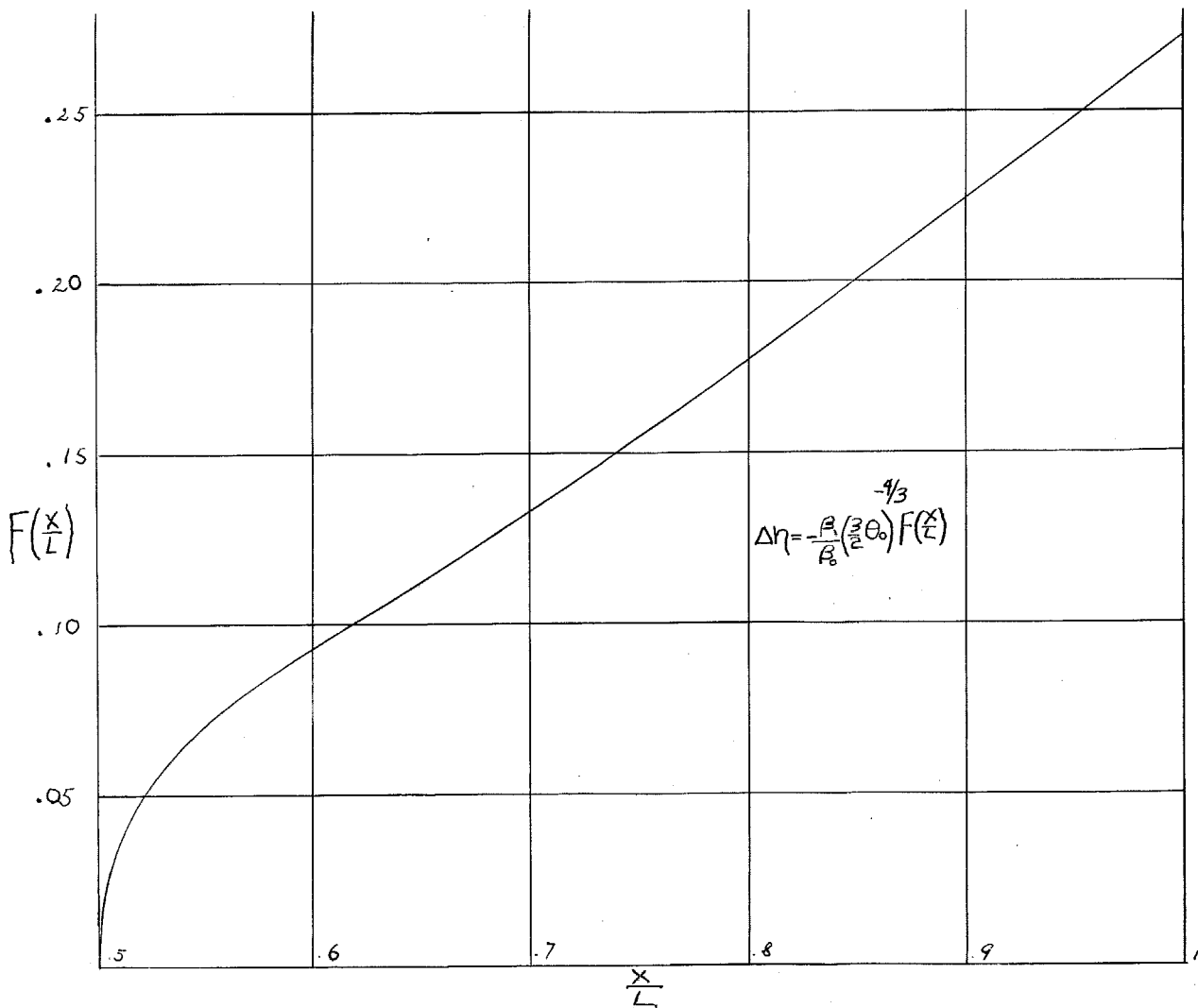
Fig. 21 $\Delta\eta$ ALONG THE REAR PART OF THE WEDGE

$c_p \cdot \theta_o^{-\frac{2}{3}}$

$g\left(\frac{x}{L}\right)$

Closed Wall Tunnel

Free Air Case